

2190

LLNL UCRL-53698
IN PRESS

**Geochemical Gradients in the Topopah Spring Member
of the Paintbrush Tuff:
Evidence for Eruption Across a Magmatic Interface**

B. C. Schuraytz¹

T. A. Vogel¹

L. W. Younker²

January 1986

¹Department of Geological Sciences, Michigan State University,
East Lansing, MI 48824.

²Earth Sciences Department, Lawrence Livermore National
Laboratory, Livermore, CA 94550.

element composition and estimated quench temperatures, and thus are chemically similar to their associated whole-rock tuff composites. In contrast, the chemical variability among pumices within the uppermost quartz latite is as great as that of the entire ash-flow sheet. The top of the flow consists of both high- and low-silica pumices with significant differences in trace element abundance and estimated quench temperature among the various pumice lumps.

The heterogeneity among pumices in the Topopah Spring Member can be explained by a model in which the angular velocity field developed near the entrance region of the vent results in simultaneous withdrawal of magma from a continually greater lateral and vertical extent within the chamber. The relative chemical homogeneity within the high-silica rhyolite tuff suggests that the chemical gradients within the high-silica rhyolitic magma were either modest or that this layer was efficiently mixed during eruption. The abrupt transition to chemically variable pumices, dominated by those of quartz latitic composition, implies that the interface between the magma layers remained relatively stable until drawdown breached the interface and preferentially erupted higher temperature, more mafic magma along with subordinate amounts of the incompletely exhausted high-silica rhyolitic magma.

CONTENTS

Introduction	1
General Geologic Relations	6
The Topopah Spring Member	7
Methods	11
Sample Selection	11
Analytical Procedure	14
Results	16
Major Element Chemistry	16
Trace Element Chemistry	21
Coexisting Fe-Ti Oxides and Estimated Temperatures	24
Other Mineral Variations	32
Discussion	34
Origin of the Pumice Heterogeneity	34
Hypothesis of a Liquid-liquid Interface	38
Conclusions	42
Acknowledgments	42
References Cited	43
Table 1: Accuracy and Precision of Analytical Data	48
Table 2: Major and Trace Element Chemical Analyses	49
Table 3: Summary of Phenocryst Data	61
Figure Captions	62
Figures 1-13	64
Appendix 1	78

INTRODUCTION

The common occurrence of systematic compositional and mineralogical zonations within ash-flow sheets provides strong evidence that their source magma bodies were chemically and thermally zoned (for a review see Smith, 1979; Hildreth, 1981; Mahood, 1981; Bacon et al., 1981; Crecraft et al., 1981; Baker and McBirney, 1985). Recently, interest in how zoned magmas evolve and erupt has focused on the fluid dynamic aspects of magma chambers. The results of scaled laboratory experiments using aqueous solutions have been used to suggest that the interfacial effects of compositionally and thermally contrasting fluid layers may be important in the differentiation of magmas (Huppert and Sparks, 1984; Sparks et al., 1984; Huppert et al., 1984; McBirney et al., 1985; Baker and McBirney, 1985). Theoretical studies of magma withdrawal during eruption indicate that magma from different depths within the chamber will erupt simultaneously and that ash-flow stratigraphy will not simply represent the inverse of the zonations within the magma body (Blake, 1981; Spera, 1984). The purpose of this study is to evaluate key assumptions and predictions of these fluid dynamic models using geochemical data obtained from pumice from a well known zoned ash-flow sheet -- the Topopah Spring Member of the Paintbrush Tuff. The specific questions addressed herein are: to what degree does the compositional zonation in the Topopah Spring Member represent the inverse of the compositional zonation in the magma body and was the zonation in the magma body characterized by continuous gradients within a single liquid or by discontinuous gradients within discrete

liquid layers separated by a distinct interface. A major emphasis of this study is placed on the heterogeneities among pumices that have been observed within all stratigraphic horizons throughout the ash-flow sheet. With few exceptions (Lipman, 1967; Byers et al., 1968; Noble et al., 1969; Rose et al., 1979; Wright and Walker, 1977), this important feature has received sparse attention in previous studies.

It has long been realized that ash-flow tuffs and associated calderas result from the explosive eruption and partial evacuation of large volumes of magma at single points in time (Williams, 1941; Smith, 1960) and that the chemical and mineralogical variability of these tuffs may be used to infer pre-eruptive magmatic conditions. Among the first to establish this premise was the study by Lipman et al. (1966) of the Topopah Spring Member of the Paintbrush Tuff. A notable feature of this voluminous ash-flow sheet is the systematic variation in composition with stratigraphic height. The zonation from nearly aphyric high-silica rhyolite upward into phenocryst-rich quartz latite was first described by Lipman et al. (1966) and interpreted by them to reflect the compositional zonation of magma in the source chamber prior to eruption.

Subsequent studies of this (Noble and Hedge, 1969; Lipman, 1971; Lipman and Friedman, 1975) and other compositionally variable ash-flow sheets have provided a considerable base of chemical, isotopic, and mineralogical data (for a review see Hildreth, 1981; Baker and McBirney, 1985). This information has been used to estimate compositional and thermal gradients inferred to be present in the magma chambers. It is these inferred gradients that are

fundamental in evaluating various magmatic differentiation mechanisms thought to operate in high-level magmatic systems. The importance of precise reconstruction of the eruptive sequence (and the inferred thermo-chemical gradients) cannot be overemphasized if quantitative tests of differentiation mechanisms are to lead to meaningful conclusions.

It is axiomatic that a stratigraphic sequence preserves depositional order. This fact combined with the progressive compositional variation observed in ash-flow sheets promotes the tacit assumption that "These systems are normally tapped from the top down." (Smith, 1979, p. 18). That is, the lowermost portions of the erupted sequence are derived from the upper part of the magma chamber and overlying products are derived from successively deeper levels. For example, Cox et al. (1979) state that "It is essential, in order that the evidence be preserved, that the eruption is not accompanied by excessive mixing of magma from different parts of the chamber. That zoned magma chamber sequences exist at all implies also a lack of convection in the chamber." (Cox et al., 1979, p. 273). This is undoubtedly true with regard to large scale convection, and it should be noted that the authors of the above statement were aware of additional complexities and limitations (Cox et al., 1979, p. 275).

The complexities and limitations referred to above are discussed in a detailed study of an ash-flow sheet from the Aso caldera, Japan (Lipman, 1967). Lipman demonstrated that bulk compositions of these tuffs deviate significantly from original magmatic compositions due to eruption, emplacement, and post-emplacement processes. He cited

as evidence both chemical and mineralogical heterogeneities within and among individual pumice. These features, and the conclusions Lipman drew from them, clearly indicate the need to understand the dynamic processes involved in ash-flow eruptions in order to properly assess the primary character of their quenched products.

Recent interest in the fluid-dynamical processes involved in high-level magmatic systems has prompted research concerning input and replenishment of magma (Richelberger, 1980; Huppert and Sparks, 1980; Huppert and Turner, 1981; Huppert et al., 1982b, 1984), internal magmatic differentiation processes (Chen and Turner, 1980; Huppert et al., 1982a; McBirney and Noyes, 1979; Sparks et al., 1984; Turner and Gustofson, 1981; Turner et al., 1983; McBirney et al., 1985; Baker and McBirney, 1985), and dynamics associated with eruption and magma withdrawal (Wilson et al., 1980; Blake, 1981; Blake and Ivey, 1984; Spera, 1983, 1984; Schuraytz et al., 1983; Wohletz et al., 1984).

The Topopah Spring Member of the Paintbrush Tuff is a classic example of a compositionally zoned ash-flow sheet for which the field relations are well constrained and for which substantial documentation of characteristic features is available. This study presents new major and trace element chemical analyses and iron-titanium oxide phenocryst analyses, primarily from samples of glassy pumice. The purpose of these analyses is to determine if there were continuous gradients or discrete, discontinuous zones in the magma body that erupted the Topopah Spring Member. A recurring theme throughout this paper is the nearly ubiquitous occurrence of

chemical heterogeneities among individual pumice. While this feature may be a hindrance in that it may obscure primary magmatic variations, it also provides information that can be used to evaluate dynamic processes associated with petrogenesis.

GENERAL GEOLOGIC RELATIONS

The Topopah Spring Member is the lowermost formal unit of the Paintbrush Tuff, a major effusive sequence associated with the Timber Mountain-Oasis Valley caldera complex in southern Nye County, Nevada (Byers et al., 1976). This caldera complex is a major part of the southwestern Nevada volcanic field which was active during the upper Tertiary period. Eruptive activity occurred contemporaneously with extensional basin-range normal faulting (Christiansen et al., 1965; Lipman et al., 1966; Ekren et al., 1968; Christiansen et al., 1977). The Timber Mountain-Oasis Valley caldera complex is comprised of four overlapping and superposed volcanic centers (Byers et al., 1976), recording evidence of repeated eruptive activity of a high-level magmatic system from 16 to 9 m.y. ago (Kistler, 1968; Marvin et al., 1970).

The Paintbrush Tuff consists of genetically related bedded tuff and ash-flow tuff sheets that were erupted 13.2-12.5 m.y. ago from the Claim Canyon cauldron center,* the southernmost part of which is exposed in an arcuate segment along the south side of the Timber Mountain-Oasis Valley caldera complex (Byers et al., 1976). In ascending stratigraphic order, the four major units of the Paintbrush Tuff are the Topopah Spring, Pah Canyon, Yucca Mountain, and Tiva

* Christiansen et al. (1977) present the alternative view that the Yucca Mountain and Tiva Canyon Members may have been erupted from an overlapping area including the Oasis Valley cauldron segment, centered slightly northwest of the Claim Canyon segment; however, the Claim Canyon segment did subside during eruption of the Tiva Canyon Member.

Canyon Members. Both the Topopah Spring and Tiva Canyon Members, which are the most voluminous ash-flow sheets, are compositionally zoned from high-silica rhyolite to quartz latite.* In contrast, the Pah Canyon and Yucca Mountain Members are volumetrically smaller by several orders of magnitude and lack extensive compositional zoning. The Pah Canyon Member is lithologically similar to the quartz latitic caprock of the Topopah Spring Member and the Yucca Mountain Member consists of uniform high-silica rhyolite similar to that at the base of the overlying Tiva Canyon Member. These four ash-flow sheets and associated lavas record repeated volcanic activity of a single evolving magma chamber that was part of a larger high-level magmatic system. In this context, the Topopah Spring Member represents the tapping of this chamber during a relative "instant", early in its evolution.

The Topopah Spring Member

The Topopah Spring Member is a multiple-flow compound cooling unit that is inferred to have originally covered an area of 1,800 km², with an extracauldron volume of 170 km³ (Lipman et al., 1966). An unknown volume of tuff, inferred to be buried beneath

* The compositional designation of quartz latite and the term caprock synonymously refer to the uppermost subunit of the eruptive sequence, that is more mafic and crystal-rich than the underlying subunits, and commonly forms an erosion resistant ledge (Lipman et al., 1966; Byers et al., 1976). However, Christiansen et al. (1977) point out that this uppermost subunit contains a much lower Ca/(Na+K) ratio than typical quartz latites and plots in the rhyolite field of the classification scheme of O'Connor (1965).

the Claim Canyon cauldron, led Byers et al. (1976) to suggest that the total eruptive volume was probably greater than 250 km³. Estimate of the total eruptive volume, however, has been recently revised upward to 1,200 km³ (Scott et al., 1984; F. M. Byers, Jr., personal commun., 1985), making the Topopah Spring Member the most voluminous ash-flow sheet of the Paintbrush Tuff. Figure 1 is a map of the inferred distribution and thickness of the Topopah Spring Member.

Field relations and characteristic lithologic and petrographic features of the Topopah Spring Member have been thoroughly described by Lipman, Christiansen, and O'Connor (1966). Because the majority of samples analyzed in the present study were collected from outcrops that have been previously described, only a brief summary of the characteristic features noted by Lipman et al. (1966, p. F5-11) is presented here. The Busted Butte section (fig. 1) is representative of the Topopah Spring Member and serves to illustrate the zonal variations in composition, welding, and crystallization.

At Busted Butte, the base of the ash-flow sheet directly overlies genetically related bedded ash-fall material and consists of a 3 meter thick zone of light colored nonwelded pumice and ash. Above this zone, there is a gradational increase in the degree of welding with increasing stratigraphic height which is evident by the presence of collapsed pumice and darkening of the shard matrix. This zone grades upward into a 15 meter thick densely welded vitrophyre in which the pumice, occurring as black fiamme, contrast against the dark grey shard matrix. There is an abrupt transition at the top of this lower vitrophyre into overlying densely welded crystalline

(devitrified) tuff. Above this transition is approximately 14 meters of densely welded devitrified tuff that contains several lithophysal zones and in which two depositional contacts between flow units have been identified. The 170 meter thickness of tuff described thus far constitutes approximately 90 percent of the total thickness of the Busted Butte section. This entire thickness is composed of high-silica rhyolite (77-74% SiO₂) which contains a major phenocryst assemblage of alkali feldspar, plagioclase, biotite, and opaque oxides that increases uniformly upward from approximately 1 to 6 percent. Within the next 5 meters, there is a progressive change from rhyolite to quartz latite along with a considerable increase in the percentage of phenocrysts. In the remaining 15 meters, the total phenocryst assemblage increases to about 21 percent with the addition of minor amounts of clinopyroxene, quartz, and hornblende, and the whole-rock silica content decreases to approximately 69 weight percent. Approximately 4 meters above the transition to quartz latite, there is an abrupt change from devitrified tuff to a 3 meter thick upper vitrophyre. The upper vitrophyre grades upward into partly welded and nonwelded tuff, where the upper contact of the Topopah Spring Member is sharply overlain by ash-fall material.

The thicknesses of these various subunits vary laterally throughout the ash-flow sheet and several distinct subunits that are recognized at other localities (e.g., the xenolithic subunit at Black Glass Canyon) are absent from the Busted Butte section (Lipman et al., 1966). As noted by Lipman et al. (1966), these variations are probably due to both the progressive change in the composition of the

erupted magma and the mechanical processes of eruption and emplacement.

In this study, an attempt was made to evaluate the vertical and lateral compositional variations within the Topopah Spring Member by sampling sections that were widely separated and that spanned the entire range in thickness. However, for reasons discussed in the following section, chemical analyses were performed primarily on samples from the upper and lower margins of measured sections.

METHODS

Sample Selection

Because precise reconstruction of thermo-chemical gradients inferred to be present within the magma chamber is crucial to the evaluation of differentiation mechanisms, two primary considerations guided the sampling scheme in this study. First and foremost was the desire to sample individual glassy pumices, based on the assumption that these samples most closely preserve the composition of the magma, with the exception that volatiles have been lost. In contrast, whole-rock tuff samples represent composite mixtures that are subject to sorting and xenolithic contamination during eruption, transportation, and deposition. Although vitric samples were preferred over samples which have undergone vapor phase crystallization and devitrification, it has been shown that even glassy samples have usually been chemically modified as a result of secondary ground water hydration and no longer strictly represent the composition of magmatic liquids (Aramaki and Lipman, 1965; Lipman, 1965; Noble, 1965; 1967). Second, was the desire to obtain samples from sections where the entire eruptive sequence was preserved and close stratigraphic control could be maintained, so that the relative position of samples in the magma chamber could be more readily inferred. This consideration was based on the assumption that the compositional zonation of magma within the source chamber is preserved in inverted sequence in the ash-flow sheet.

It is usually difficult to satisfy the above criteria within the same measured section. The nature of the densely welded devitrified interior of thick sections precludes obtaining glassy pumices from

the central portion of the eruptive sequence in sections where the entire sequence is present. Glassy pumices are generally confined to the nonwelded to partly welded margins and densely welded vitrophyres. The abundance and size of the pumices also vary vertically in the section (Lipman et al., 1966); however, this is partly due to the effects of welding and devitrification which often obscure the compacted pumice lenses. Although pumices are readily distinguishable in vitrophyres, their compacted nature makes removal quite tedious and sometimes futile.

In the theoretical, ideal case, where a given stratigraphic horizon of the ash-flow sheet corresponds to a single stratigraphic level in the magma chamber, the thermo-chemical gradients in the pre-eruptive magma may be reconstructed by randomly sampling individual pumice, vertically throughout the eruptive sequence. However, with respect to the Topopah Spring Member, it is clearly evident that more than one type of pumice is present within a small volume of tuff at any given stratigraphic horizon. The variability among pumice types is readily distinguishable by textural characteristics, most notably those of color, phenocryst content, and vesicular structure. At the base of the ash-flow sheet, at least five distinct pumice types can be recognized within an area of 200 cm² (fig. 2a) and several other pumices with textural characteristics intermediate to these occur within close proximity. None of the pumice observed are distinctly banded or display other macroscopic features indicative of commingling. With increasing stratigraphic height, fewer distinct pumice types are recognizable, as welding tends to obscure the primary textural features. However,

individual pumices clearly display a differential response to welding that, in some cases, appears to be independent of size or orientation. At the top of the ash-flow sheet, the number of pumice types is similar to that at the base, although the nature of the textural distinctions are more clearly attributable to differences in phenocryst abundance and vesicularity, as well as color. This marked textural heterogeneity among individual pumice is illustrated in figure 2.

This pumice heterogeneity has important implications that necessarily influenced the sampling strategy. On the basis of megascopic textural differences among pumices, without addition of chemical and mineralogical data, it is only possible to conclude that the various pumice types have had different histories. Because these differences may or may not correspond to compositional differences (primary or secondary), discussion of hypotheses for the origin of the pumice heterogeneity is deferred until the chemical analyses of the individual pumice have been presented. In order to evaluate this feature, however, each pumice type must be considered separately. Each section was measured at vertical intervals of 1.5 meters, beginning at clearly defined contacts with underlying or overlying ash-fall material. At each interval that was sampled, all in situ, macroscopically distinct pumice types were collected, in addition to a large block of whole-rock tuff which contained the various pumice types. For reasons previously noted, the preponderance of individual glassy pumices selected for analyses were collected within 3 meters of the upper and lower margins of the ash-flow sheet. Several glassy fiamme and whole-rock tuff samples

were also analyzed in order to achieve some degree of continuity throughout the eruptive sequence and to compare the compositions of individual pumice with their whole-rock tuff composite mixtures. Every effort was made to perform all analyses on single whole pumices. In some cases, this was not possible because there was insufficient mass from the small sized pumice to perform ICP, INAA, and heavy mineral separation on a single pumice. However, it is possible to distinguish the various pumice types by textural features such as structure of vesicles, glass color, and phenocryst content. Only pumices that were texturally identical were combined. 18 of the 50 pumice samples represent composites of texturally identical pumices and these samples are indicated in the data tables. The data base comprises samples collected from outcrops at the Busted Butte, 311 Wash, and Lathrop Wells sections, and from drill hole USW-GU3, the locations of which are shown in figure 1. The stratigraphic positions of individual samples and their relation to zones of bulk composition, crystallization, and welding are illustrated in figure 3.

Analytical Procedure

Fifty whole pumice and 22 whole-rock tuff samples were analyzed in this study. After coarse crushing, the fine fraction was examined petrographically for secondary carbonate, and if calcite was observed, the samples were leached in a mixture of sodium acetate and glacial acetic acid. The samples were then pulverized by hand in an agate mortar. All samples were analyzed by instrumental neutron activation analysis (INAA) at Lawrence Livermore National Laboratory

and by inductively coupled plasma emission spectroscopy (ICP) at Barringer Magenta, LTD. Results of analyses of U.S.G.S. standards BCR-1 and GSP-1, which were analyzed as unknowns, are reported alongside their published values in table 1.

There was sufficient material from 52 samples to concentrate phenocrysts for microprobe analysis. Heavy minerals from the -60+140 sieve size fraction were separated in bromoform and mounted in epoxy. Analyses of Fe-Ti oxide and selected silicate phenocrysts were collected using a JEOL 733 automated electron microprobe at Lawrence Livermore National Laboratory. Oxide and silicate standards were used for quantitative analysis with the Bence-Albee correction procedure (Bence and Albee, 1968).

RESULTS

Major Element Chemistry

The major element oxide analyses are reported in table 2. For purposes of discussion and graphical presentation, all values have been recalculated to 100 weight percent excluding loss on ignition (LOI), to facilitate comparison between variably hydrated glassy and devitrified samples. The overall range and trend in major element composition of the Topopah Spring Member was first reported by Lipman et al. (1966), based on 13 whole-rock tuff samples and one densely welded crystallized pumice. The additional analyses reported in this study are consistent with those provided by Lipman et al. (1966), and also help to clarify the previously addressed question regarding an apparent compositional gap. More important, these additional analyses demonstrate that the textural heterogeneity of pumices observed in the field corresponds to chemical heterogeneities among the pumices, with a systematic variation in their compositional range with stratigraphic position in the ash-flow sheet.

Figure 4 illustrates the variation of the major elements with stratigraphic height in the ash-flow sheet at each sample location. Considering only the whole-rock tuff samples from the Busted Butte section (fig. 4a), SiO_2 displays a total variation from 77.9 wt. % near the base to 68.5 wt. % near the top, with a pronounced chemical change to lower values of SiO_2 coincident with the transition from crystal-poor tuff to crystal-rich caprock (Lipman et al., 1966). However, the various pumices occurring at a given stratigraphic level display a range in SiO_2 . At the base of the ash-flow sheet, all pumices are high-silica rhyolites, and although individual pumices

have marked textural variations, they display only a modest range in SiO_2 content. In contrast, the range in SiO_2 for pumice at the top of the ash-flow sheet is nearly as great as that of the entire section. At this stratigraphic level, there is a compositional variation among pumices ranging from high-silica rhyolite to quartz latite (76.2-67.7 wt. %). Although no attempt was made to quantify the proportions of the different pumice types at a given stratigraphic level, comparison of the compositions of the various pumices with their associated whole-rock tuff composites gives a first approximation of their relative abundances. It must be noted, however, that while sufficiently large whole-rock tuff samples were taken and their lithic fragments removed before powdering, only one whole-rock tuff sample was taken at a given stratigraphic level.

Unfortunately, due to the difficulty of removing pumice from the densely welded central portion of the ash-flow sheet, it was not possible to fully evaluate the degree of chemical heterogeneity at every stratigraphic level within the entire eruptive sequence. Although the textural variations of pumice lenses in the densely welded devitrified horizons are less extreme, careful observations allow subtle distinctions among pumice to be made at most stratigraphic levels. Based on data from other pumices and the overall chemical similarity of whole-rock tuff samples within the crystal-poor rhyolite, any compositional differences corresponding to these textural differences are likely to be modest as well.

The relationship described for SiO_2 at the Busted Butte section has corresponding variations for all the major oxides and at all sample localities. It is apparent from figure 4 that the chemical

compositions of individual pumices within a given stratigraphic level are not unique, but display a range in composition. Moreover, it is apparent that pumices with compositions similar to those deposited during the early phase of the eruption are present throughout the eruptive sequence. The range in pumice compositions increases with increasing stratigraphic height; however, due to the paucity of pumice analyses from the central portion of the ash-flow sheet, the progressive nature of this increase in range is uncertain. This chemical heterogeneity has profound implications for the reconstruction of inferred chemical gradients in the magma chamber based on ash-flow stratigraphy.

The interelement variation of the major oxides with weight percent silica is depicted in figure 5. The solid symbols represent analyses of whole pumice whereas the open symbols represent whole-rock tuff samples. The overall trends are consistent with the data reported by Lipman et al. (1966). In these previously published analyses (diamond shaped symbols), no data points occur in the interval from 71.8 to 74.7% SiO_2 . This apparent gap was thought to be real (Hildreth, 1981) and has been interpreted to indicate the existence of a sharp compositional interface or a narrow transition zone within the magma chamber. The additional analyses reported in this study show an overall continuity in the variation of SiO_2 , although compositions in this aforementioned interval are significantly under represented. The paucity of compositions in this interval may be due to inadequate sampling of the central portion of the eruptive sequence, because three of the six samples that occur in this interval are from the interior of the sequence.

Alternatively, it may be that the occurrence of compositions in this interval is the result of limited mixing between compositionally contrasting magmas.

This latter view is supported by several lines of evidence. Four of the six samples in this interval are whole-rock tuff samples that contain more than one pumice type, and therefore do not represent the composition of a single parcel of magmatic liquid. The two pumice samples in this compositional interval were collected from the very top of the distal portion of the ash-flow sheet and occur alongside both more silicic and more mafic pumice, and thus their relative position in the magma chamber is uncertain; they may represent either mixed liquids or fractionates resulting from differentiation processes occurring near a compositional interface. In spite of the absence of a distinct compositional gap, the hypothesis of the existence of a sharp magmatic interface or a narrow transition zone is consistent with the slope of the interelement variation trends. From figure 5, it is apparent that the major oxide trends are not strictly linear, but display a somewhat dichotomous distribution with a change in abundance occurring within the interval of the previously noted gap at approximately 74% SiO₂. This is best illustrated by the oxides Fe₂O₃(T), TiO₂, and P₂O₅. The more abundant high-silica rhyolites (>75% SiO₂) do appear to define linear trends, generally having little scatter and showing very slight variation of the corresponding major elements with increasing SiO₂; this latter feature may be an artifact of the constant sum effect. Notable exceptions are the alkalis which may be mobilized during

secondary hydration (Aramaki and Lipman, 1965; Lipman, 1965; Noble, 1965; 1967). Although there is a greater density of data points in the high-silica group, these analyses represent an equal number of samples from the upper and lower horizons of the ash-flow sheet.

These trends can be interpreted to indicate that high-silica rhyolitic magma was separated from underlying low-silica rhyolitic magma by a distinct compositional interface within a single magma body, and that two compositionally distinct magmas evolved concomitantly.

Trace Element Chemistry

Highly charged trace elements, particularly the rare earth elements (REE), are especially useful in evaluating petrogenetic models because they often display relatively large variations in abundance within coeval rocks that have only a modest range in major element composition. In the Topopah Spring Member, there is a strong correlation between the abundance of certain trace elements and major element concentrations. The chemical heterogeneity among pumice that is observed with the major elements is also observed with the trace elements. These data further support the hypothesis that a sharp compositional interface or narrow transition zone existed between chemically distinct magmas within a single source chamber. Trace element abundances of samples analyzed in this study are presented in table 2.

Figure 6a illustrates the variation in the abundance of 7 rare earth elements for all samples of the Topopah Spring Member. The ordinate value is the ratio of the concentration of an element in the sample to the average concentration of that element in chondrites reported by Haskin et al. (1968). With the exception of one whole-rock tuff sample (CP4-60WR), indicated by the dashed line, there is a lack of intermediate concentrations for the elements La, Ce, and Eu, which allows two major groups of REE patterns to be distinguished. Within each of the two groups, the individual patterns illustrate continuous variation, and most patterns within each group are subparallel, indicating an overall coherence in REE distribution. Several samples, however, have patterns that display a cross-over near Sm, with slight LREE depletion and corresponding HREE enrichment, similar to that observed in the Bishop Tuff (Hildreth, 1977).

The REE patterns that lie above the trend of CP4-60WR (fig. 6b) generally correspond to samples of low-silica rhyolite (quartz latite) and all of these samples occur in stratigraphic units that lie above CP4-60WR in the ash-flow sheet. Within this group, the negative Eu anomaly progressively diminishes to predicted values, as the LREE concentration increases, with up to seven times the L concentration of the high-silica pumices. The REE patterns that lie below the trend of CP4-60WR (fig. 6c) correspond to samples of high-silica rhyolite. These exhibit relatively little variation and are characterized by large negative Eu anomalies and maximum LREE enrichment of approximately 140 times chondritic abundances. In contrast to the LREE enriched samples, pumice samples that exhibit these trends occur throughout the ash-flow sheet. The REE patterns of individual samples in relation to their stratigraphic positions in the ash-flow sheet are illustrated in figure 7.

This systematic chemical heterogeneity among pumices, which is most pronounced at the top of the ash-flow sheet, is demonstrable for nearly all elements that have a significant range in concentration (see table 2). Rather than plotting all the trace elements versus stratigraphic position, it is useful to consider the covariation of selected trace elements for which a large variation has been established.

* The predicted Eu concentration, Eu^* , is that calculated by linear extrapolation between the chondrite normalized concentrations of Sm and Tb on a plot of REE concentration versus atomic number.

In figure 8, various trace elements are plotted against SiO_2 to illustrate their behavior with increasing differentiation. The elements Ba, Sr, Eu, Zr, and La, all decrease with increasing SiO_2 . These trends are consistent with control by fractionation of alkali feldspar, plagioclase, zircon, and chevkinite/perrierite, phases that are petrographically observed in the low-silica samples. In contrast, the elements Ta, Rb, Cs, Th, and Sb display incompatible behavior, all increasing with SiO_2 . A significant feature common to all elements in fig. 8 is a marked change in concentration at approximately 74% SiO_2 , similar to that observed for the major element oxides. To illustrate that this rather abrupt change in elemental concentrations is not solely an artifact of the non-linear behavior of SiO_2 , several of these elements are plotted against each other in figure 9. The trends of Ta, Rb, Ba, and Hf vs. Th all display apparent inflections for the same concentration of Th, although the changes in slope are less drastic for the incompatible elements Ta and Rb. Trends of compatible vs. incompatible elements (i.e., Ba vs. Rb) or of two elements that are compatible with different phases (i.e., Ba vs. Zr) generally show greater changes in slope.

Coexisting Iron-titanium Oxides and Estimated Temperatures

In conceptual models of magma chambers, probably the least equivocal assumption is that the temperature of magma increases with depth in the chamber. In contrast, the assumption that the composition of magma becomes more mafic with depth in the chamber is largely based on inference from the overall whole-rock compositional variation with stratigraphic height within ash-flow sheets. Although this last assumption is considered quite reasonable, previous sections of this paper present clear evidence that pumice compositions, which most closely represent quenched parcels of magmatic liquid, do not strictly become more mafic with increasing stratigraphic height in the Topopah Spring Member. Therefore, it is desired to isolate some other position dependent parameter that can be used to constrain chemical gradients within the magma chamber. For reasons discussed above, the quenched equilibrium temperature of liquidus phases would appear to be a logical choice.

In order to employ the iron-titanium oxide geothermometer and oxybarometer of Spencer and Lindsley (1981), heavy mineral separates from 52 samples were prepared for microprobe analyses and 50 samples contained both magnetite and ilmenite phenocrysts. In many of these samples, either the magnetite or ilmenite or both display visible exsolution lamellae. The term 'exsolution' used herein refers to the occurrence of $\text{Ilm-Hem}_{\text{SS}}$ along {111} cubic spinel planes due to oxidation of $\text{Usp-Mt}_{\text{SS}}$, and the occurrence of $\text{Usp-Mt}_{\text{SS}}$ along {0001} rhombohedral planes due to reduction of $\text{Ilm-Hem}_{\text{SS}}$. These processes of oxidation (and reduction) generally take place at temperatures above 600° C (Haggerty, 1976, p. 18). As pointed out

by Buddington and Lindsley (1964), this is not true exsolution in the classic sense but has been adopted for lack of a better term. Some grains also display oxidation to maghemite and hematite along grain margins and fractures, possibly due to ground water movement through the ash-flow sheet (Lipman, 1971). These grains were not considered for analyses.

Previous workers tried to minimize problems of subsolidus oxidation and unmixing during devitrification by studying Fe-Ti oxide phenocrysts only from glassy rocks (Carmichael, 1967; Lipman, 1971; Hildreth, 1977). Hildreth (1977) suggested that the exsolved oxide phenocrysts in the Bishop Tuff possibly resulted from protracted cooling in fully crystalline welded zones or were due to emplacement over wet ground of the nonwelded basal portions. However, even when only glassy rocks were considered (i. e., comparison of nonwelded basal pumice with densely welded vitrophyre), Lipman (1971) noted that there seemed to be little correlation between degree of oxidation of magnetite phenocrysts and cooling history.

Although post-emplacement processes were no doubt operative to some extent in the Topopah Spring Member (Lipman, 1971), the following evidence is used to suggest that exsolution may have resulted from dynamic processes occurring within the magma chamber prior to or concomitant with eruption: (1) several individual pumices contain both unexsolved and exsolved oxide phenocrysts; (2) entirely vitric pumices from the nonwelded top and base of the ash-flow, which may have been emplaced over wet ground but were certainly not subjected to slow cooling, contain both unexsolved and exsolved oxide phenocrysts; (3) samples from the central fully crystalline (devitrified) welded zone, where protracted cooling is unequivocal,

contain both unexsolved and exsolved oxide phenocrysts. Any secondary alteration process, occurring outside the magma chamber and operating on a local scale (pumice or handsample), should effect all oxide phenocrysts of the same composition more or less equally. If any such process is argued to be compositionally selective, then the presence of variably effected phenocrysts is strong evidence for primary compositional differences. Although the possibility of xenocrystic contamination during emplacement must be considered for whole-rock tuff samples, this problem is avoided for individual pumice samples (Lipman, 1971).

Therefore, the exsolved Fe-Ti oxide phenocrysts in the Topopah Spring Member are interpreted to reflect disequilibrium within the magma chamber. Because the compositions of Fe-Ti oxides are extremely sensitive to changes in temperature and oxygen fugacity of the surrounding silicate liquid, if the thermal regime is perturbed, the composition of the phenocrysts will change toward equilibrium with the ambient conditions. For example, during mechanical mixing or convection, magma parcels of greatly contrasting composition and temperature are juxtaposed and may commingle. If mixing is sluggish and the thermal regime changes gradually, zoned phenocrysts may result. However, if disruption of equilibrium occurs suddenly during vigorous mixing of relatively short duration, these oxide phenocrysts may respond by internal exsolution. Carmichael (1967) cites evidence that suggests the Fe-Ti oxides do not rapidly re-equilibrate to a change in environment, and interaction between these phenocrysts and the silicate liquid may be assumed to cease at the time the liquid is quenched. Therefore, with the assumption that exsolution only

effects an internal rearrangement of these oxide phenocrysts, rather than a change in bulk mineral composition, it should be possible to assess the bulk composition of a single grain..

Several previous studies have attempted to obtain bulk analyses of exsolved Fe-Ti oxide phenocrysts. In a study of Fe-Ti oxides from compositionally zoned ash-flow sheets in southwestern Nevada (Lipman, 1971), which included four reported temperatures for the Topopah Spring Member, bulk compositions of exsolved phenocrysts were obtained by separate microprobe analyses of both the exsolved lamellae and the surrounding matrix. These analyses were then combined based on estimation of the relative contribution of each to the total area of the phenocryst. Rutherford and Hemming (1978) rejected wet chemical analysis because it was apparent that more than one composition of titanomagnetite occurred in the rocks under investigation and that these phenocrysts contained abundant inclusions. Their solution was to use the scanning capability of the microprobe to analyze several sufficiently large areas across individual grains.

In this study, the method used was similar to that employed by Rutherford and Hemming (1978). Multiple analyses were collected along a trace across each grain, where each analysis was performed by rastering the microprobe beam over an area of $100\mu^2$. This posed a problem in some cases because the Bence-Albee correction program used in the data reduction (Bence and Albee, 1968) assumes homogeneity of the area being analyzed. This resulted in poor totals for chemical analyses of inhomogeneous regions. Because the microprobe can only determine total iron, which is reported as FeO, it is necessary to

compute a value for Fe_2O_3 in order to recast the analyses into stoichiometric oxide minerals and to assess the quality of the analyses (Carmichael, 1967). Because analyses on unexsolved oxide phenocrysts invariably yielded excellent totals, and determinations on the standard both before and after each analytical session were reproducible, the recalculated totals provide some indication of the degree of exsolution within the analyzed area.

On the average, five grains each of magnetite and ilmenite were analyzed for each sample, with an average of three analyses per phenocryst. In some highly exsolved phenocrysts, as many as 10 analyses were performed. All multiple analyses of single grains were averaged. With few exceptions, unexsolved phenocrysts were internally homogeneous and unzoned, so that averaging of multiple analyses merely increases the precision with which the bulk composition can be reported. For the exsolved phenocrysts, it was assumed that averaging of multiple analyses yields the closest approximation to the bulk composition of the grain prior to exsolution. Those analyses that could not be recast into a stoichiometric oxide phase or that yielded recalculated totals less than 95 weight percent were rejected from further consideration. The remaining data set consists of ilmenite and magnetite analyses from 46 samples, of which 25 are from individual pumice (Appendix 1).

In order to strictly employ the ilmenite-magnetite geothermometer to yield an estimated quench temperature for an individual pumice, it is necessary to demonstrate that a single pair of ilmenite and magnetite phenocrysts and their surrounding glass coexisted in mutual equilibrium at the time of eruption. This requirement would

generally be satisfied if a single composition of magnetite and ilmenite were present within a sample. The range of 2σ uncertainties in temperature and oxygen fugacity of the solution model of Spencer and Lindsley (1981) is reported assuming $\pm 1\%$ uncertainties in Usp_{ss} and Ilm_{ss} compositions. This is interpreted to mean that if the compositional uncertainties in Usp_{ss} and Ilm_{ss} are $\leq 1\%$ within a single sample, then a single population of magnetite and ilmenite may be assumed. However, in the Topopah Spring Member, the average uncertainties in the mole fractions of Usp_{ss} and Ilm_{ss} within a sample are approximately 3%. It is not clear whether this variation is due to the presence of multiple magnetite and/or ilmenite populations within a sample, or whether this variation is an artifact of averaging analyses from exsolved phenocrysts. As it is not possible to resolve this dilemma with the available data, the estimated temperatures and oxygen fugacities presented herein are intended as approximations only. All respective ilmenite and magnetite analyses within a sample have been averaged to yield an ilmenite-magnetite pair for each sample. This approach is not totally without precedent. In a discussion of coexisting iron-titanium oxides of salic volcanic rocks, Carmichael (1967) states that "As there is little to no zoning in all the oxide minerals, the bulk analysis derived from the probe data of between 15 and 20 grains should very closely approximate to their bulk

composition." (Carmichael, 1967, p. 43). Although Carmichael was not referring to exsolved phenocrysts, the intra-sample variation in this study is of the same or smaller order of magnitude.

Figure 10 illustrates the range in estimated quench temperature and oxygen fugacity for the samples of the Topopah Spring Member based on the mean composition of ilmenite and magnetite phenocryst within a sample. Also included are four data points recalculated from analyses previously published by Lipman (1971). These temperatures and oxygen fugacities were calculated according to the method of Spencer and Lindsley (1981) using a modified Fortran version of their computer program TFO2. The mole fractions of ilmenite and ulvospinel were calculated according to the method prescribed by Stormer (1983), using a modified Fortran version of his computer program OXYCALC2. This latter program also calculates mole fraction values according to the schemes suggested by Carmichael (1967), Anderson (1968), and Spencer and Lindsley (1981). The deviation among these various methods has been thoroughly discussed by Stormer (1983). For the samples considered in this study, the difference in the calculated temperature and oxygen fugacity using the various methods is invariably less than the estimated mode errors including the 2 σ compositional uncertainty.

The data in figure 10 show nearly continuous variation from approximately 620 to 1000° C. Within this range, however, there appears to be a dichotomous distribution of the glassy pumice (solid symbols), evident by the paucity of data in the interval from 805 to 883° C. Two pumice samples yield somewhat higher estimated quench temperatures of 1126 and 1149° C, respectively.

As one might predict from the extreme chemical heterogeneity among pumices within the uppermost horizon of the ash-flow sheet, the estimated quench temperatures of individual pumices at this level span the entire temperature range of the eruptive sequence. Figure 11 illustrates this variation in estimated quench temperature with stratigraphic height at each of the sample locations. The open symbols, which represent samples of whole-rock tuff, show relatively little variation in quench temperature throughout the crystal-poor rhyolite, with a notable increase within the crystal rich caprock. Thus, the degree of heterogeneity in the compositions of the iron-titanium oxides and their respective temperatures, within and among pumices at a given stratigraphic horizon, correlate fairly well with the chemical heterogeneity at the same level.

Figure 12 illustrates the variation of several trace elements and SiO_2 with estimated quench temperature. All the trace elements show similar trends when plotted against SiO_2 (fig. 8), but opposite in direction. There is considerably greater scatter in the distribution of these elements for estimated quench temperatures above 800°C . This appears to distinguish two populations corresponding to the high-silica rhyolite and lower silica quartz latite samples. This is most clearly illustrated by the solid symbols which represent the glassy pumice samples. As noted previously, these two populations are more pronounced for the compatible elements and these elements are more abundant in the quartz latite. It is also apparent that the two somewhat higher estimated temperatures of 1126 and 1149°C correspond to pumices that are among the most mafic in composition.

Other Mineral Variations

Apart from the Fe-Ti oxides, analyses of phenocrysts from the Topopah Spring Member collected in this study are limited to partial analyses of several samples from the same outcrop in the upper portion of the section at 311 Wash. These data are briefly summarized in table 3. Although a comprehensive study of the phenocryst mineralogy of the pumice is lacking at this time, the limited analyses presented here do provide some indication of phenocryst heterogeneity within pumices. A single high-silica rhyolite pumice from this uppermost flow unit (CP3-1C) contains plagioclase and alkali feldspar phenocrysts that vary over a significant compositional range. Admittedly, the limited data from these few samples do not allow any firm conclusions, however, they do lend some support to the inference that the greater compositional variations in the Fe-Ti oxides in pumices from the top of the ash-flow sheet may reflect mixing of compositionally distinct magmas from different levels in the magma chamber.

Several other studies that include phenocryst data from the Topopah Spring Member suggest that the compositional variations of liquidus phases resulted from growth in a magma that was compositionally zoned prior to the onset of crystallization. Lipman et al. (1966) noted that although there is a striking variation in phenocryst content between the high-silica rhyolite and quartz latitic tuff, most of the compositional variation is due to differences in groundmass composition. They also noted the presence of minor amounts of clinopyroxene and trace amounts of hornblende in the quartz latite, phases that are distinctly absent in the high-

silica rhyolite (Lipman et al., 1966). Significant variations in the compositions of biotite, plagioclase, and sanadine between the upper and lower units of the Topopah Spring Member have recently been documented by Warren et al. (1984) and Broxton et al. (1985). There are also differences in the REE phases between the lower and upper units. Scott et al. (1984) have shown that the REE phase in the rhyolitic units is allanite, whereas in the quartz latitic units the REE phase is perrierite/chevkinite.

DISCUSSION

Origin of the Pumice Heterogeneity

The chemical, mineralogical, and textural heterogeneity among pumices in the Topopah Spring Member clearly emphasizes the importance of the scale of observation when evaluating petrogenetic processes. On the scale of a hand sample of whole-rock tuff, the progressive variation from crystal-poor high-silica rhyolite to crystal-rich quartz latite with increasing stratigraphic height was inferred to reflect the trend toward increasingly more mafic, crystal-rich, high temperature magma with depth in the chamber (Lipman et al., 1966). On the scale of individual pumices, however, the relationship between stratigraphic position in the ash-flow sheet and depth in the magma chamber needs to be re-evaluated because there is a variation in the compositions and estimated quench temperatures among pumices at a given stratigraphic level. This compositional and textural heterogeneity is inferred to result from simultaneous eruption of compositionally contrasting magma from different parts of a magma chamber that was systematically zoned with respect to composition and temperature. Not only is there a host of evidence from other ash-flow sheets that indicates depth dependent compositional and thermal gradients within magma chambers, but the theoretical fluid dynamic regime of magma withdrawal from a zoned magma chamber predicts that in most cases, the chamber will not be simply emptied in a layer cake fashion. For example, Blake (1981) comments that this view that ash-flow sheets simply represent inverted magma bodies is too simplistic because this would require an

unrealistic flow pattern of magma removal. Blake (1981) approached the problem by a mathematical analysis of the removal of magma from a chamber by applying the solution of Weissberg (1962) for the velocity field within a large flat-topped reservoir as a fluid flows upward into a cylindrical conduit. If the diameter of the conduit is considerably smaller than the diameter of the reservoir, fluid will approach the conduit from all directions in a radial fashion, not just from directly below it. At large horizontal distances from the conduit, the radial component of fluid velocity is small in comparison to that directly below the conduit. Hence, the net, or angular velocity field developed near the entrance region to the conduit results in a parabolic velocity profile composed of hyperbolic streamlines along which fluid accelerates towards the conduit (Blake, 1981). By considering this velocity profile, one can determine the sub-circular locus of points within the fluid reservoir that will reach the conduit entrance at the same time. This hyperbolic profile, or 'eruption isochron', as defined by Blake (1981), relates position within the reservoir to time of entrance in the conduit for a given eruptive volume. General theoretical solutions describing the dynamics of magma withdrawal and the geometries of evacuation isochrons for assumed boundary conditions have been presented by Blake (1981), Blake and Ivey (1984), and Spera (1983, 1984).

Figure 13 is a highly schematic cross-sectional cartoon that illustrates the general model of a zoned magma body as proposed by Smith (1979), on which several hypothetical eruption isochrons have been superposed. Admittedly, this depiction is a gross

oversimplification, as the actual shapes of the 3-dimensional hyperbolic surfaces will be governed by the geometries of the conduit and reservoir and the physical properties of the magma. For example, eruption through a ring fracture system, which is more appropriate for the Topopah Spring Member, would be better approximated by a toroidal evacuation isochron with a large width to depth ratio. It is also apparent from geologic field evidence that the conduit plumbing systems of large caldera forming ash flows do not remain constant during the course of eruption. Precise mathematical modeling of the evacuation isochrons for these complex and transient geometries can quickly become intractable. The more immediate goal of this study is to show that the chemical heterogeneity of pumice in the Topopah Spring Member is consistent with the qualitative predictions of the general fluid dynamic models.

Figure 13 shows several of an infinite number of evacuation isochrons that could be considered from the onset to the final phase of eruption, with that representing the final phase having a volume equal to the total volume of the eruption. Each successive evacuation isochron will draw magma from progressively deeper levels at the expense of magma near the roof of the chamber. However, as illustrated by the largest isochron in figure 13, magma near the roof of the chamber is not completely exhausted but is continually erupted along with magma from all levels down to the deepest level tapped. Assuming that the magmatic gradients change monotonically with depth in the chamber, each successive isochron will sample magma of progressively greater differences in chemical and physical properties. Thus, the fluid dynamic model for eruption from a zoned

magma chamber predicts that successive volumes of magma leaving the vent will be composite mixtures of magma with increasingly heterogeneous bulk properties.

The geochemical data from both the whole-rock tuff and whole pumice samples are consistent with this model for subterranean eruption dynamics. The whole-rock tuff samples, which become more mafic with increasing stratigraphic height in the ash-flow sheet, represent the bulk composition of a given eruption isochron and are composite mixtures of quenched magma from various positions within the magma chamber. The whole pumice samples, which span a progressively greater compositional range with increasing stratigraphic height in the ash-flow sheet, represent the composition of quenched parcels of magma from various positions along the periphery of an evacuation isochron.

There are several alternative mechanisms that might give rise to compositional heterogeneity within a 'depositional isochron'. For example, several ash flows that erupt from laterally separated vents that extend to different depths in the magma chamber could coalesce during emplacement to produce a composite mixture of compositionally contrasting pumices. The possibility of subaerial coalescence during eruption from separate vents along the ring fracture system of the Claim Canyon caldera must be considered and obviates the need for development of criteria to distinguish between the effects of subaerial mixing and subterranean mixing in the magma chamber/vent system. However, it is emphasized that the fluid dynamic considerations discussed above would be applicable to each of the laterally separate vents or semi-continuous segments along a ring fracture system. It might also be considered that successive

portions of a turbulent ash flow could entrain and suspend pumice of different compositions as the ash flow passed over earlier erupted material. Subaerial mixing undoubtedly occurs to some extent, and may seem to be an attractive explanation for the heterogeneity among pumice, in the apparent absence of banded pumices. However, it is difficult to conceive of how pumices from the top of the ash-flow sheet, that are identical in composition and estimated quench temperature to pumices from the base of the sheet, could be continually rafted upward for the duration of the eruptive episode. Spera (1984) has noted that the time interval that a parcel of magma spends in the subaerial realm before coming to rest is on the order of 10^2 s in comparison to 10^4 - 10^5 s for the duration of an eruptive episode. Although the occurrence of banded pumices would provide favorable evidence for subterranean mixing, its apparent absence is not a severe limitation. In a study of the Black Mountain volcanics, Vogel et al. (in prep.) have documented the occurrence of unzoned, disequilibrium phenocryst assemblages within individual pumices that have homogeneous glass compositions. The limited phenocryst data presented in this study indicate that disequilibrium phenocryst assemblages within homogeneous glasses may also be significant in the Topopah Spring Member.

Hypothesis of a Liquid-liquid Interface

The geochemical data from whole glassy pumices further constrain the inferred chemical and thermal gradients within the pre-eruptive magma chamber. In contrast to the whole-rock tuff samples, which are composite mixtures of compositionally heterogeneous pumices, the

pumice samples define trends that display abrupt changes in slope on interelement variation diagrams and apparent compositional gaps for certain elements. Because the pumice samples from the uppermost horizon of the ash-flow sheet span the entire range in major and trace composition and estimated quench temperature, these gaps do not appear to be an artifact of inadequate sampling of pumices from the central portion of the eruptive sequence. Rather, these gaps and abrupt changes in elemental concentrations are inferred to reflect the changes in composition and temperature across a liquid-liquid interface between chemically and thermally contrasting magmas within a single chamber (Schuraytz et al., 1985).

This hypothesis of a liquid-liquid interface within the magma body is further supported by the abrupt increase in phenocryst content at the transition from rhyolite to quartz latite in the ash-flow sheet. Previous interpretation of this lithologic feature (Lipman et al., 1966) concluded that the abrupt change in crystal content did not result from downward settling of phenocrysts from the rhyolitic magma and simple accumulation in the erupted part of the quartz latitic magma. Because most of the chemical variation is due to differences in groundmass composition, they inferred that crystallization occurred in place within a magma body that was chemically zoned in the liquid state. The more advanced stage of crystallization in the lower, quartz latitic part of the magma chamber, in spite of its higher temperature, could be explained by an increased water content in the upper part of the magma chamber resulting in a lowering of the liquidus temperature. However, as this change in crystal content is more abrupt than gradational, this

feature is re-interpreted in light of recent theoretical and experimental fluid dynamic studies.

Theoretical interpretation of the occurrence of mafic inclusions in silicic lavas (Eichelberger, 1980) and laboratory models of replenished magma chambers have illuminated a host of fluid dynamic phenomena that can result when a relatively hot, compositionally dense liquid is injected below a cooler, less dense liquid (Huppert and Sparks, 1980; Huppert and Turner, 1981; Huppert et al., 1982b, 1984; McBirney et al., 1985; Baker and McBirney, 1985).

Of particular interest is a recent experiment (Huppert et al., 1984) in which the viscosity of the cooler and compositionally less dense upper layer was considerably greater than that of the hotter and denser layer below. An immediate effect of this thermally unstable situation is the growth of crystals in the lower layer at the interface due to heat transfer to the upper layer. Crystallization in the lower layer causes the surrounding fluid to become less dense and this less dense fluid was released immediately and continuously from the interface into the overlying layer with no significant mixing. By varying the initial conditions of temperature, composition, viscosity, and configuration of the various fluid layers, Huppert et al. (1984) have observed numerous double-diffusive effects of relevance to magmatic processes.

The discontinuous chemical gradients and abrupt change in phenocryst content in the Topopah Spring Member are consistent with a model in which a distinct liquid-liquid interface separated relatively high temperature, phenocryst-rich quartz latite from overlying lower temperature, phenocryst-poor high-silica rhyolite in

a single magma chamber. The geochemical data from this ash-flow sheet should provide useful boundary conditions for the evaluation of double-diffusive phenomena in a particular geologic system.

CONCLUSIONS

The magmatic gradients inferred from chemical analyses and estimated quench temperatures of whole glassy pumices from the Topopah Spring Member indicate that the transition from high-silica rhyolitic to quartz latitic magma within the chamber was abrupt, rather than gradational, with a distinct liquid-liquid interface separating the two contrasting magmas. Concomitant with eruption, this interface was disrupted, causing magma of contrasting composition and temperature to erupt simultaneously. Although limited mixing may have occurred as a result of a convergent flow regime, the duration of the eruption interval was not sufficient to produce a completely homogeneous magma. This is supported by textural and chemical heterogeneity among pumice within stratigraphic horizons of the ash-flow sheet and implies that the Topopah Spring Member does not reflect a "simple" inverse stratigraphy of the chemical zonation of magma in the source chamber.

ACKNOWLEDGMENT

This work has been supported by the Nuclear Test Containment Program at Lawrence Livermore National Laboratory.

REFERENCES

- Abbey, S., Calibration standards, X-Ray Spectrometry, 7, 99-121, 1978.
- Anderson, A. T., Oxidation of the La Blache Lake titaniferous magnetite deposit, Quebec, J. Geol., 76, 528-547, 1968.
- Aramaki, S., and P. W. Lipman, Possible leaching of Na₂O during hydration of volcanic glasses, Japan Acad. Proc., 41, 467-470, 1965.
- Bacon, C. R., R. Macdonald, R. L. Smith, and P. A. Baedeker, Pleistocene high-silica rhyolites of the Coso volcanic field, Inyo County, California, J. Geophys. Res., 86, 10223-10241, 1981.
- Baker, B. H., and A. R. McBirney, Liquid fractionation. Part III: Geochemistry of zoned magmas and the compositional effects of liquid fractionation, J. Volcanol. Geotherm. Res., 24, 55-81, 1985.
- Bence, A. E., and A. L. Albee, Empirical correction factors for the electron microanalyses of silicates and oxides, J. Geol., 76, 382-403, 1968.
- Blake, S., Eruptions from zoned magma chambers, J. Geol. Soc. London, 138, 281-287, 1981.
- Blake, S., and G. N. Ivey, Magma mixing and the dynamics of withdrawal from stratified reservoirs, Proc. Conf. Open Magmatic Systems, 13-15, 1984.
- Broxton, D. E., F. M. Byers, Jr., and R. G. Warren, Trends in phenocryst chemistry in the Timber Mountain-Oasis Valley volcanic field, SW Nevada: Evidence for episodic injection of primitive magma into an evolving magma system (abstract), Geol. Soc. Am. Abstr. Programs, 17, 345, 1985.
- Buddington, A. F., and D. H. Lindsley, Iron-titanium oxide minerals and synthetic equivalents, J. Petrol., 5, 310-357, 1964.
- Byers, F. M., Jr., W. J. Carr, P. P. Orkild, W. D. Quinlivan, and K. A. Sargent, Volcanic suites and related cauldrons of Timber Mountain-Oasis Valley caldera complex, southern Nevada, U. S. Geol. Surv. Prof. Pap. 919, 70 pp., 1976.
- Byers, F. M., Jr., P. P. Orkild, W. J. Carr, and W. D. Quinlivan, Timber Mountain Tuff, southern Nevada, and its relation to caldron subsidence, in Nevada Test Site, edited by E. B. Eckel, Mem. Geol. Soc. Am., 110, 87-97, 1968.
- Carmichael, I. S. E., The iron-titanium oxides of silic volcanic rocks and their associated ferromagnesian silicates, Contrib. Mineral. Petrol., 14, 36-64, 1967.

- Chen, C. F., and J. S. Turner, Crystallization in a double-diffusive system, J. Geophys. Res., **85**, 2573-2593, 1980.
- Christiansen, R. L., P. W. Lipman, W. J. Carr, F. M. Byers, Jr., P. P. Orkild, and K. A. Sargent, Timber Mountain-Oasis Valley caldera complex of southern Nevada, Geol. Soc. Am. Bull., **88**, 943-959, 1977.
- Christiansen, R. L., P. W. Lipman, P. P. Orkild, and F. M. Byers, Jr., Structure of the Timber Mountain caldera, southern Nevada, and its relation to Basin-Range structure, U. S. Geol. Surv. Prof. Pap. 525-B, B43-B48, 1965.
- Cox, K. G., J. D. Bell, and R. J. Pankhurst, The Interpretation of Igneous Rocks, 450 pp., George Allen & Unwin, London, 1979.
- Crecraft, H. R., W. P. Nash, and S. H. Evans, Jr., Late Cenozoic volcanism at Twin Peaks, Utah; Part I: Geology and petrology, J. Geophys. Res., **86**, 10303-10320, 1981.
- Eichelberger, J. C., Vesiculation of mafic magma during replenishment of silicic magma reservoirs, Nature, **288**, 446-450, 1980.
- Ekren, E. B., C. L. Rogers, R. E. Anderson, and P. P. Orkild, Age of basin and range normal faults in Nevada Test Site and Nellis Air Force Range, Nevada, in Nevada Test Site, edited by E. B. Eckel, Mem. Geol. Soc. Am., **110**, 247-250, 1968.
- Flanagan, F. J., U. S. Geological Survey standards-II. First compilation of data for the new U. S. G. S. rocks, Geochim. Cosmochim. Acta, **33**, 81-120, 1969.
- Haggerty, S. E., Opaque mineral oxides in igneous rocks, in Oxide Minerals, edited by D. Rumble III, Mineral. Soc. Am. Short Course Notes, pp. Hg-101-300, 1976.
- Haskin, L. A., M. A. Haskin, F. A. Frey, and T. R. Wildeman, Relative and absolute terrestrial abundances of the rare earths, in Origin and Distribution of the Elements, edited by L. H. Ahrens, pp. 889-912, Pergamon Press, New York, 1968.
- Hildreth, E. W., The magma chamber of the Bishop Tuff: Gradients in temperature, pressure, and composition, Ph.D. thesis, 328 pp., Univ. Calif., Berkeley, 1977.
- Hildreth, W., Gradients in silicic magma chambers: Implications for lithospheric magmatism, J. Geophys. Res., **86**, 10153-10192, 1981.
- Huppert, H. E., and R. S. J. Sparks, The fluid dynamics of a basaltic magma chamber replenished by influx of hot dense ultrabasic magma, Contrib. mineral. Petrol., **75**, 279-289, 1980.
- Huppert, H. E., and R. S. J. Sparks, Double-diffusive convection due to crystallization in magmas, Ann. Rev. Earth Planet. Sci., **12**, 11-37, 1984.

- Huppert, H. E., and J. S. Turner, A laboratory model of a replenished magma chamber, Earth Planet. Sci. Lett., 54, 144-152, 1981.
- Huppert, H. E., R. S. J. Sparks, and J. S. Turner, Effects of volatiles on mixing in calc-alkaline magma systems, Nature, 297, 554-557, 1982a.
- Huppert, H. E., J. S. Turner, and R. S. J. Sparks, Replenished magma chambers: Effects of compositional zonation and input rates, Earth Planet. Sci. Lett., 57, 345-357, 1982b.
- Huppert, H. E., R. S. J. Sparks, and J. S. Turner, Some effects of viscosity on the dynamics of replenished magma chambers, J. Geophys. Res., 89, 6857-6877, 1984.
- Kistler, R. W., Potassium-argon ages of volcanic rocks in Nye and Esmeralda Counties, Nevada, in Nevada Test Site, edited by E. B. Eckel, Mem. Geol. Soc. Am., 110, 251-263, 1968.
- Lipman, P. W., Chemical comparison of glassy and crystalline volcanic rocks, Geol. Soc. Am. Spec. Pap., 82, 260-261, 1965.
- Lipman, P. W., Mineral and chemical variations within an ash-flow sheet from Aso caldera, southwestern Japan, Contrib. mineral. Petrol., 16, 300-327, 1967.
- Lipman, P. W., Iron-titanium oxide phenocrysts in compositionally zoned ash-flow sheets from southern Nevada, J. Geol., 79, 438-456, 1971.
- Lipman, P. W., and I. Friedman, Interaction of meteoric water with magma: An oxygen-isotope study of ash-flow sheets from southern Nevada, Geol. Soc. Am. Bull., 86, 695-702, 1975.
- Lipman, P. W., R. L. Christiansen, and J. T. O'Connor, A compositionally zoned ash-flow sheet in southern Nevada, U. S. Geol. Surv. Prof. Pap. 524-F, 47 pp., 1966.
- Mahood, G. A., A summary of the geology and petrology of the Sierra La Primavera, Jalisco, Mexico, J. Geophys. Res., 86, 10137-10152, 1981.
- Marvin, R. F., F. M. Byers, Jr., H. H. Mehnert, P. P. Orkild, and T. W. Stern, Radiometric ages and stratigraphic sequence of volcanic and plutonic rocks, southern Nye and western Lincoln Counties, Nevada, Geol. Soc. Am. Bull., 81, 2657-2676, 1970.
- McBirney, A. R., and R. M. Noyes, Crystallization and layering of the Skaergaard intrusion, J. Petrol., 20, 487-554, 1979.
- McBirney, A. R., B. H. Baker, and R. H. Nilson, Liquid fractionation. Part I: Basic principles and experimental simulations, J. Volcanol. Geotherm. Res., 24, 1-24, 1985.

- Noble, D. C., Ground-water leaching of sodium from quickly cooled volcanic rocks, (abstract), Am. Mineral., 50, 289, 1965.
- Noble, D. C., Sodium, potassium, and ferrous iron contents of some secondarily hydrated natural silicic glasses, Am. Mineral., 52, 280-286, 1967.
- Noble, D. C., and C. E. Hedge, Sr⁸⁷/Sr⁸⁶ variations within individual ash-flow sheets, U. S. Geol. Surv. Prof. Pap. 650-C, 133-139, 1969.
- Noble, D. C., J. C. Drake, and M. K. Whallon, Some preliminary observations on compositional variations within the pumice- and scoria-flow deposits of Mount Mazama, Proc. Andesite Conf. State of Oregon Dept. Geol. Min. Ind., 157-164, 1969.
- O'Connor, J. T., A classification for quartz-rich igneous rocks based on feldspar ratios, U. S. Geol. Surv. Prof. Pap. 525-B, B79-B86, 1965.
- Rose, W. I., Jr., N. K. Grant, and J. Easter, Geochemistry of the Los Chocoyos Ash, Quezaltenango Valley, Guatemala, Geol. Soc. Am. Spec. Pap., 180, 87-99, 1979.
- Rutherford, N. F., and R. F. Hemming, The volatile component of Quaternary ignimbrite magmas from the North Island, New Zealand, Contrib. Mineral. Petrol., 65, 401-411, 1978.
- Schuraytz, B. C., T. A. Vogel, and L. W. Younker, Pumice heterogeneity in the Topopah Spring Member of the Paintbrush Tuff: Implications for ash-flow eruption dynamics (abstract), Eos Trans. AGU, 64, 896, 1983.
- Schuraytz, B. C., T. A. Vogel, and L. W. Younker, Inflections in elemental and mineralogical gradients within the Topopah Spring Member of the Paintbrush Tuff: Evidence for the resolution of compositional and thermal properties across a magmatic interface, (abstract), Eos Trans. AGU, 66, 391, 1985.
- Scott, R. B., F. M. Byers, Jr., and R. G. Warren, Evolution of magma below clustered calderas, southwest Nevada volcanic field (abstract), Eos Trans. AGU, 65, 1126-1127, 1984.
- Smith, R. L., Ash flows, Geol. Soc. Am. Bull., 71, 795-842, 1960.
- Smith, R. L., Ash-flow magmatism, Geol. Soc. Am. Spec. Pap., 180, 5-27, 1979.
- Sparks, R. S. J., H. E. Huppert, and J. S. Turner, The fluid dynamics of evolving magma chambers, Phil. Trans. R. Soc. London, A 310, 511-534, 1984.
- Spencer, K. J., and D. H. Lindsley, A solution model for coexisting iron-titanium oxides, Am. Mineral., 66, 1189-1201, 1981.

- Spera, F. J., Simulations of magma withdrawal from crustal reservoirs (abstract), Eos Trans. AGU, 64, 876, 1983.
- Spera, F. J., Some numerical experiments on the withdrawal of magma from crustal reservoirs, J. Geophys. Res., 89, 8222-8236, 1984.
- Stormer, J. C., Jr., The effects of recalculation on estimates of temperature and oxygen fugacity from analyses of multicomponent iron titanium oxides, Am. Mineral., 68, 586-594, 1983.
- Turner, J. S., and L. B. Gustafson, Fluid motions and compositional gradients produced by crystallization or melting at vertical boundaries, J. Volcanol. Geotherm. Res., 11, 93-125, 1981.
- Turner, J. S., H. E. Huppert, and R. S. J. Sparks, An experimental investigation of volatile exsolution in evolving magma chambers, J. Volcanol. Geotherm. Res., 16, 263-277, 1983.
- Warren, R. G., F. M. Byers, Jr., and F. A. Caporuscio, Petrography and mineral chemistry of units of the Topopah Spring, Calico Hills, and Crater Flat tuffs, and older volcanic units, with emphasis on samples from drill hole USW G-1, Yucca Mountain, Nevada Test Site, Rep. LA-10003-MS, 78 pp., Los Alamos Nat. Lab., Los Alamos, N. M., 1984.
- Weissberg, H. L., End correction for slow viscous flow through long tubes, Phys. Fluids, 5, 1033-1036, 1962.
- Williams, H., Calderas and their origin, Univ. of California Publications in Geological Sciences, 25, 239-346, 1941.
- Wohletz, K. H., T. R. McGetchin, M. T. Sandford II, and E. M. Jones, Hydrodynamic aspects of caldera-forming eruptions: Numerical models, J. Geophys. Res., 89, 8269-8285, 1984.
- Wright, J. V., and G. P. L. Walker, The ignimbrite source problem: Significance of a co-ignimbrite lag-fall deposit, Geology, 5, 729-732, 1977.

TABLE 1. U.S.G.S. standards analyzed as unknowns compared with published concentrations (Abbey, 1978).

A. Concentrations of U.S.G.S. standard GSP-1 determined by inductively coupled plasma emission spectroscopy (ICP).

(Wt. %)	Abbey (1978)	ICP	% difference
SiO ₂	67.31	67.7	-0.58
Al ₂ O ₃	15.19	15.2	-0.07
Fe ₂ O ₃ (T)	4.33	4.23	2.31
CaO	2.02	2.05	-1.49
MgO	.96	1.07	-11.46
TiO ₂	.66	.59	10.61
MnO	.04	.04	0.00
Na ₂ O	2.80	2.96	-5.71
K ₂ O	5.53	5.06	8.50
P ₂ O ₅	.28	.35	-25.00
(ppm)			
Be	1.5	1.1	26.67
V	49	51	-4.08
Ni	9	10	-11.11
Cu	35	33	5.71
Zn	98	107	-9.18
Sr	230	247	-7.39
Ba	1300	1220	6.15
Pb	53	50	5.66

B. Concentrations of U.S.G.S. standard BCR-1 determined by instrumental neutron activation analysis (INAA).

(ppm)	Abbey (1978)	INAA	% difference	% stand. dev.	n
Sc	34	34	0.00	4.24	7
Cr	16	17	-6.25	6.84	7
Co	37	39	-5.41	4.18	7
Rb	47	54	-14.89	5.93	7
Zr	185	169	8.65	14.60	6
Sb	.6	.7	-16.67	6.78	7
Cs	.95	.98	-3.16	7.21	7
La	25	27	-8.00	3.54	7
Ce	54	54	0.00	6.59	7
Nd	29	27	6.90	12.85	4
Sm	6.6	6.4	3.03	6.77	7
Eu	1.9	2.0	-5.26	3.19	7
Tb	1.0	1.0	0.00	6.63	7
Yb	3.8	3.6	5.26	9.14	7
Lu	.6	.5	16.67	8.23	6
Hf	4.5	5.4	-20.00	5.55	7
Ta	.88*	0.78	11.36	6.09	7
Th	6.0	5.7	5.00	6.99	7
U	1.8	1.9	-4.56	22.30	7

*Flanagan (1969).

TABLE 2. CHEMICAL ANALYSES OF WHOLE PUMICES AND WHOLE-ROCK TUFFS OF THE TOPOPAH SPRING MEMBER.

Major element oxides have been recalculated to 100% water free. Locations of samples (see fig. 1) indicated by two letter prefix: BB = Busted Butte; CP = 311 Wash; LW = Lathrop Wells; Gu = Drill Hole USW-GU3. 'WR' suffix in field no. indicates whole-rock tuff. An asterisk indicates a combined sample of texturally identical pumices. All other samples are individual whole pumice.

SAMPLE#	1	2	3	4	5	6
FIELD#	BB9-1WR	BB9-1A*	BB9-1B*	BB9-1C*	BB9-5C*	BB9-10A*
(WT. %)						
SiO ₂	70.5	75.9	69.6	70.7	69.2	76.2
Al ₂ O ₃	13.8	12.6	15.9	15.7	15.8	12.2
Fe ₂ O ₃	1.60	1.48	2.12	1.99	2.20	.90
CaO	4.07	.10	.56	.50	1.27	.65
MgO	.31	.07	.40	.42	.42	.12
TiO ₂	.30	.10	.47	.44	.47	.11
MnO	.08	.05	.13	.11	.09	.02
Na ₂ O	3.28	3.47	4.09	4.03	4.43	3.35
K ₂ O	5.98	6.22	6.52	6.01	5.91	6.42
P ₂ O ₅	.09	.02	.13	.11	.13	.03
(PPM)						
BE	2.2	1.9	2.7	3.1	1.8	2.4
SC	5	2	7	7	7	3
V	11	10	17	16	13	3
CR	-	-	3	-	4	-
CO	.4	.1	.5	.6	.5	.2
NI	<1	<1	<1	<1	2	<1
CU	5	10	3	4	4	4
ZN	78	19	121	124	82	31
RB	154	171	148	151	138	175
SR	116	15	179	149	203	28
ZR	391	138	699	603	732	143
SB	.3	.4	.4	.3	.1	.3
CS	3.96	4.61	3.14	3.39	2.62	4.02
BA	1390	117	2910	2230	2350	160
LA	113	31	200	185	217	48
CE	170	70	320	321	360	101
ND	61	31	104	93	100	37
SM	9.2	5.8	12.5	11.8	13.2	6.3
EU	1.6	.2	3.2	2.7	3.6	.4
TB	.8	.7	.9	.9	.9	.8
YB	2.8	3.1	3.2	3.3	3.1	2.9
LU	.6	.6	.5	.5	.5	.6
HF	8.8	5.0	14.9	11.9	14.9	5.8
TA	.98	1.35	.77	.87	.80	1.29
PB	30	25	40	40	15	5
TH	19.7	22.7	19.9	18.9	20.3	25.1
U	4.6	4.7	2.9	5.0	2.8	5.0

SAMPLE# FIELD#	7 BB9-10C*	8 BB9-15WR	9 BB9-25WR	10 BB8-320WR	11 BB8-200WR	12 BB8-100WR
(WT. %)						
SiO2	67.7	68.6	68.5	75.6	76.2	76.7
Al2O3	16.0	15.9	16.2	12.8	12.3	12.3
Fe2O3	2.34	2.26	2.11	.99	.93	1.00
CaO	1.63	1.31	1.68	.58	.63	.55
MgO	.44	.40	.62	.09	.15	.07
TiO2	.49	.47	.37	.10	.09	.09
MnO	.10	.09	.09	.06	.11	.06
Na2O	4.49	4.66	4.98	4.08	3.94	3.98
K2O	6.75	6.19	5.39	5.59	5.63	5.18
P2O5	.15	.12	.12	.03	.01	.02
(PPM)						
BE	1.8	1.7	1.9	3.2	3.1	3.1
SC	7	7	7	2	2	2
V	14	13	10	4	4	5
CR	-	-	-	-	-	-
CO	.6	.6	.7	.2	.2	.2
NI	98	16	34	7	<1	33
CU	7	4	5	7	3	4
ZN	116	63	58	47	43	44
RB	135	126	123	180	190	202
SR	224	207	161	22	27	22
ZR	675	656	639	151	126	160
SB	.2	.1	.2	.3	.4	.4
CS	2.79	2.68	1.92	3.78	4.44	3.86
BA	2840	2420	1380	192	80	50
LA	215	201	181	34	35	34
CE	322	349	314	72	83	69
ND	108	114	97	27	26	24
SM	13.0	11.8	11.2	5.7	6.2	5.7
EU	3.7	3.4	2.9	.3	.3	.2
TB	.9	.9	.9	.8	.8	.7
YB	2.8	3.0	3.0	3.1	3.3	2.2
LU	.5	.6	.6	.5	.6	.4
HF	14.4	14.4	13.0	4.9	5.1	4.7
TA	.80	.84	.92	1.31	1.38	1.38
PB	10	20	25	45	40	25
TH	19.5	19.6	20.2	22.1	23.8	21.0
U	3.4	2.1	4.5	4.5	5.0	3.8

SAMPLE# FIELD#	13 BB8-85BWR	14 BB8-85B*	15 BB8-20	16 BB8-15B	17 BB8-15C	18 BB8-10WR
(WT. %)						
SIO2	76.4	76.9	77.0	77.0	78.2	77.9
AL2O3	13.0	12.9	12.9	13.4	12.2	12.5
FE2O3	.98	.97	.93	.99	.90	.94
CAO	.67	.66	.58	.45	.52	.64
MGO	.07	.06	.17	.21	.12	.12
TIO2	.10	.11	.12	.14	.10	.11
MNO	.07	.08	.08	.13	.07	.07
NA2O	4.49	3.58	3.23	2.90	3.23	3.04
K2O	4.12	4.67	4.96	4.68	4.63	4.66
P2O5	.03	.01	.02	.03	.03	.03
(PPM)						
BE	3.0	3.1	2.8	2.7	2.8	2.8
SC	2	2	2	2	2	2
V	3	-	2	2	2	2
CR	-	-	6	5	1	3
CO	.2	.1	.2	.8	.3	.4
NI	<1	-	6	8	6	6
CU	3	20	5	13	10	20
ZN	45	50	46	59	49	46
RB	203	235	195	194	187	186
SR	39	36	14	16	17	21
ZR	137	140	164	177	131	144
SB	.3	.4	.3	.4	.3	.4
CS	11.37	10.14	5.39	5.53	5.15	5.10
BA	42	132	27	49	27	<25
LA	38	41	34	36	33	28
CE	71	88	79	83	66	54
ND	29	35	26	26	28	26
SM	5.2	7.2	5.4	5.7	5.5	5.1
EU	.2	.3	.2	.3	.2	.2
TB	.7	.9	.7	.7	.7	.7
YB	3.0	3.4	3.0	3.1	3.1	2.8
LU	.4	.6	.5	.5	.5	.4
HF	4.8	6.0	5.4	6.4	4.9	4.9
TA	1.32	1.52	1.37	1.57	1.36	1.30
PB	20	20	25	45	25	25
TH	20.8	26.4	22.5	27.3	23.1	21.3
U	4.2	6.1	4.5	5.3	5.1	5.2

SAMPLE# FIELD#	19 BB8-10	20 BB8-5	21 BB8-3A	22 BB8-3B	23 BB8-2	24 BB8-1
(WT. %)						
SIO2	76.8	79.3	78.0	76.8	78.2	78.3
AL2O3	13.1	11.8	12.5	13.3	12.4	12.3
FE2O3	.96	.83	.87	.94	.86	.83
CAO	.85	.47	.46	.46	.49	.46
MGO	.31	.05	.10	.14	.07	.14
TIO2	.12	.09	.12	.17	.09	.11
MNO	.07	.07	.08	.06	.09	.06
NA2O	2.81	2.76	2.87	2.91	2.91	2.78
K2O	4.94	4.60	5.03	5.20	4.85	5.02
P2O5	.04	.02	.02	.02	.02	.01
(PPM)						
BE	2.8	2.8	2.8	2.8	2.9	2.8
SC	2	2	2	2	2	2
V	2	1	1	2	1	1
CR	2	2	1	2	1	1
CO	.9	.2	.3	.2	.2	.2
NI	6	6	6	6	6	6
CU	19	6	15	22	40	36
ZN	49	40	51	61	47	61
RB	192	187	205	216	188	198
SR	30	15	13	24	15	15
ZR	154	108	160	207	120	136
SB	.4	.7	.3	.3	.4	.3
CS	5.61	5.09	5.89	6.05	5.07	5.24
BA	27	27	<25	<25	27	27
LA	32	35	31	45	31	30
CE	63	82	65	92	66	57
ND	25	29	24	32	26	25
SM	5.2	5.9	5.2	6.0	5.4	5.1
EU	.2	.2	.2	.3	.2	.2
TB	.7	.8	.7	.8	.7	.6
YB	2.8	3.3	2.8	3.1	3.1	2.6
LU	.5	.3	.5	.5	.6	.4
HF	5.3	4.5	5.4	7.1	4.5	4.7
TA	1.36	1.31	1.37	1.43	1.31	1.23
PB	30	25	30	15	30	20
TH	22.2	22.0	21.8	24.2	21.6	20.3
U	4.7	5.2	4.8	5.0	4.8	4.6

SAMPLE# FIELD#	25 CP3-2A	26 CP3-2B	27 CP3-1WR	28 CP3-1A	29 CP3-1B	30 CP3-1C
(WT. %)						
SiO2	70.7	70.8	72.3	78.4	79.1	76.8
Al2O3	15.0	16.0	14.6	11.6	11.2	12.6
Fe2O3	2.27	2.12	1.69	.85	.84	.97
CaO	1.02	.31	.90	.47	.48	.49
MgO	.71	.49	.38	.08	.07	.14
TiO2	.48	.48	.35	.09	.09	.11
MnO	.09	.04	.09	.04	.03	.06
Na2O	3.85	3.58	3.94	3.30	3.11	3.34
K2O	5.78	6.11	5.69	5.11	5.03	5.49
P2O5	.12	.11	.07	.03	.02	.03
(PPM)						
BE	1.6	1.7	2.0	2.8	2.7	2.8
SC	7	7	5	2	2	3
V	12	12	8	2	1	3
CR	6	5	4	4	41	5
CO	.7	.8	.5	.2	.6	.3
NI	10	12	8	8	8	9
CU	8	15	7	6	15	8
ZN	134	390	56	40	40	49
RB	126	141	143	181	175	184
SR	188	53	61	15	14	14
ZR	717	621	463	119	125	147
SB	.2	.6	.2	.4	.4	.4
CS	4.18	4.20	3.68	5.13	4.78	5.39
BA	2880	574	574	<25	27	<25
LA	224	208	137	35	31	39
CE	372	325	233	70	58	76
ND	115	103	77	26	25	28
SM	13.2	12.4	9.7	5.5	5.1	5.8
EU	3.8	2.7	1.9	.3	.2	.3
TB	.9	.9	.9	.7	.7	.7
YB	3.2	2.8	3.0	2.9	2.7	3.0
LU	.7	.6	.6	.5	.5	.5
HF	14.8	13.0	10.1	4.6	4.7	5.1
TA	.78	.84	1.02	1.35	1.33	1.34
PB	80	575	25	25	10	35
TH	19.0	20.8	21.1	22.2	20.0	23.5
U	2.3	2.2	3.6	6.1	4.6	4.5

SAMPLE# FIELD#	31 CP3-1D	32 CP4-20BWR	33 CP4-60WR	34 CP1-3WR	35 CP1-3A	36 CP1-2E
(WT. %)						
SIO2	71.0	71.9	73.8	77.3	77.9	78.0
AL2O3	15.3	15.0	14.2	12.8	12.4	12.4
FE2O3	1.74	1.81	1.32	.94	.84	.90
CAO	.86	.87	.69	.49	.50	.45
MGO	.51	.21	.32	.18	.10	.19
TIO2	.38	.27	.19	.11	.10	.09
MNO	.09	.09	.08	.07	.07	.07
NA2O	3.57	4.44	4.43	3.43	3.37	3.03
K2O	6.48	5.32	4.98	4.71	4.68	4.85
P2O5	.08	.05	.01	.02	.02	.02
(PPM)						
BE	1.9	2.5	2.5	2.8	2.8	2.8
SC	5	4	3	3	2	3
V	7	8	5	2	1	2
CR	10	-	-	2	4	3
CO	.6	.3	.2	.2	.2	.3
NI	17	157	30	8	7	16
CU	8	7	4	6	12	6
ZN	52	51	41	52	53	52
RB	145	164	166	202	204	206
SR	43	46	35	15	14	15
ZR	431	305	220	122	121	117
SB	.2	.3	0.0	.4	.4	.4
CS	3.50	4.42	2.81	6.69	6.83	6.37
BA	314	252	152	27	<25	27
LA	163	111	70	37	33	31
CE	278	213	136	82	60	68
ND	90	67	39	30	28	23
SM	10.7	9.8	6.6	5.8	5.6	5.4
EU	2.1	1.4	.7	.3	.2	.3
TB	.9	.8	.8	.8	.7	.7
YB	3.0	3.2	2.8	3.3	2.7	3.2
LU	.6	.7	.4	.6	.5	.6
HF	10.6	9.2	6.8	5.2	4.8	5.0
TA	1.04	1.11	1.18	1.48	1.37	1.45
PB	30	25	20	30	30	20
TH	21.6	23.0	20.2	24.5	22.7	22.7
U	2.6	4.8	1.2	4.9	4.9	4.3

SAMPLE# FIELD#	37 CP1-1G	38 CP1-AFB	39 CP1-AFWR	40 LW1-A	41 LW2-A	42 LW2-5
(WT. %)						
SIO2	77.1	77.5	77.6	70.6	70.8	73.2
AL2O3	12.9	12.6	12.4	15.1	15.0	13.9
FE2O3	.90	.91	.92	1.86	1.85	1.36
CAO	.46	.44	.52	1.24	.75	.84
MGO	.10	.12	.06	.38	.38	.22
TIO2	.09	.10	.11	.43	.43	.31
MNO	.07	.08	.07	.10	.09	.09
NA2O	3.19	2.99	3.34	3.95	4.00	3.53
K2O	5.13	5.19	4.93	6.25	6.66	6.50
P2O5	.02	.02	.02	.10	.08	.06
(PPM)						
BE	2.8	2.8	2.8	1.7	1.8	2.0
SC	2	2	3	6	6	4
V	1	2	-	9	9	4
CR	1	2	2	9	6	4
CO	.2	.3	.2	1.1	.5	.5
NI	6	6	6	17	12	10
CU	5	5	6	12	8	19
ZN	49	51	52	65	63	53
RB	204	216	213	129	139	156
SR	14	12	19	61	50	31
ZR	127	126	146	564	515	397
SB	.4	.4	.4	.2	.2	.2
CS	7.43	8.38	7.71	3.31	2.96	3.46
BA	<25	27	27	391	360	102
LA	32	34	46	175	172	111
CE	66	80	91	264	310	202
ND	25	27	31	101	94	68
SM	5.6	6.0	6.1	11.7	11.8	9.4
EU	.2	.3	.3	2.2	2.3	1.2
TB	.7	.8	.8	.8	.9	.8
YB	3.0	3.4	2.8	2.9	2.8	3.0
LU	.5	.6	.5	.5	.5	.3
HF	5.0	5.6	5.2	12.0	12.0	9.8
TA	1.41	1.47	1.43	.85	.92	1.08
PB	25	20	25	20	15	15
TH	23.4	24.3	23.9	20.7	21.8	21.0
U	4.9	5.7	3.8	2.6	3.3	3.7

SAMPLE# FIELD#	43 LW2-10	44 LW4-1A	45 LW4-1B*	46 LW4-1C	47 LW4-5A*	48 LW4-5B
(WT. %)						
SIO2	78.7	77.6	73.1	70.7	78.2	71.3
AL2O3	11.4	12.0	13.9	15.0	11.6	13.9
FE2O3	.82	.92	1.38	2.18	.86	1.65
CAO	.50	.45	1.13	1.13	.68	1.55
MGO	.16	.12	.24	.20	.07	.39
TIO2	.09	.11	.27	.47	.09	.39
MNO	.05	.06	.07	.08	.05	.09
NA2O	3.14	3.39	3.37	3.85	3.26	3.75
K2O	5.14	5.32	6.38	6.22	5.18	6.82
P2O5	.03	.04	.07	.19	.04	.11
(PPM)						
BE	2.8	2.8	2.3	1.6	2.8	1.7
SC	2	2	3	7	2	5
V	2	3	7	13	3	9
CR	9	1	2	4	1	5
CO	.3	.2	.6	1.1	.3	.7
NI	13	8	9	10	8	8
CU	8	12	22	12	8	30
ZN	39	45	57	66	37	60
RB	189	183	161	134	190	136
SR	13	27	42	90	20	64
ZR	112	137	279	618	149	501
SB	.3	.4	.3	.3	.4	.4
CS	5.06	4.83	4.08	3.99	5.19	2.77
BA	<25	<25	107	1030	25	316
LA	30	39	93	215	33	152
CE	60	73	163	324	61	268
ND	26	29	50	110	26	82
SM	5.3	5.7	8.0	13.0	6.0	10.3
EU	.2	.4	1.0	2.8	.2	2.1
TB	.7	.7	.8	.9	.7	.8
YB	2.9	2.9	3.1	3.2	2.9	3.0
LU	.4	.5	.6	.6	.5	.6
HF	4.6	4.9	8.4	12.8	4.6	11.3
TA	1.35	1.29	1.10	.82	1.34	.87
PB	35	25	20	25	30	25
TH	22.0	21.7	20.9	20.5	22.0	19.7
U	5.2	5.1	4.0	2.1	4.9	2.5

SAMPLE# FIELD#	49 LW4-10A	50 LW4-10B	51 LW4-15A	52 LW4-15B	53 LW4-15C	54 GU3-31BWR
(WT. %)						
SIO2	77.1	70.9	77.5	77.8	70.1	74.9
AL2O3	11.6	14.6	11.0	11.6	15.0	13.6
FE2O3	.83	1.59	.78	.81	2.01	1.41
CAO	1.40	1.58	2.07	.93	1.55	.61
MGO	.31	.34	.41	.15	.46	.19
TIO2	.11	.36	.09	.10	.43	.23
MNO	.05	.09	.04	.06	.09	.08
NA2O	3.39	4.34	3.24	3.34	4.57	4.54
K2O	5.12	6.15	4.80	5.24	5.68	4.37
P2O5	.05	.09	.05	.05	.14	.04
(PPM)						
BE	2.5	1.8	2.5	2.7	1.6	1.7
SC	3	5	2	2	6	5
V	3	8	3	2	9	4
CR	4	-	3	3	2	-
CO	.4	.6	.5	.4	.7	.3
NI	8	8	24	8	8	<1
CU	20	23	14	9	18	3
ZN	46	64	40	39	74	58
RB	172	156	163	181	123	195
SR	47	86	50	30	203	87
ZR	145	487	120	153	659	447
SB	.4	.3	.4	.4	.2	.7
CS	4.63	3.07	4.79	4.93	2.73	3.12
BA	80	214	<25	<25	2690	805
LA	43	138	28	37	196	109
CE	82	247	56	74	291	190
ND	31	80	23	23	111	71
SM	5.5	10.3	4.8	5.3	12.3	9.2
EU	.5	1.8	.2	.3	3.3	1.5
TB	.7	.9	.7	.7	.9	.9
YB	2.8	3.0	2.8	3.1	3.1	3.6
LU	.5	.5	.5	.5	.5	.8
HF	5.2	11.3	4.5	5.0	13.8	9.7
TA	1.26	.94	1.25	1.30	.78	1.35
PB	25	20	20	25	25	65
TH	20.6	20.4	20.8	22.0	18.4	25.8
U	4.6	3.1	4.7	5.2	2.8	2.4

SAMPLE# FIELD#	55 GU3-31AWR	56 GU3-29WR	57 GU3-28WR	58 GU3-23WR	59 GU3-21WR	60 GU3-20WR
(WT. %)						
SIO2	75.0	76.0	75.4	74.8	71.9	78.4
AL2O3	13.8	12.7	13.4	13.0	15.0	12.0
FE2O3	1.36	1.41	1.42	1.57	1.83	1.02
CAO	.65	.84	.77	.75	.70	.49
MGO	.20	.19	.19	.24	.34	.13
TIO2	.23	.22	.21	.28	.37	.11
MNO	.07	.08	.08	.08	.10	.06
NA2O	4.35	4.26	4.40	4.60	4.76	4.07
K2O	4.23	4.24	4.05	4.69	4.88	3.71
P2O5	.06	.05	.06	.06	.07	.01
(PPM)						
BE	2.1	2.4	2.5	2.1	1.8	2.9
SC	5	4	4	5	6	3
V	4	5	5	7	9	3
CR	-	-	-	-	-	-
CO	.4	.3	.3	.3	.4	.1
NI	<1	2	<1	<1	<1	<1
CU	3	3	2	2	3	2
ZN	59	42	59	55	122	46
RB	192	173	177	154	155	192
SR	78	79	71	47	58	19
ZR	363	339	357	411	541	109
SB	.5	.3	.3	0.0	.4	.3
CS	3.04	5.66	3.63	2.72	4.40	3.74
BA	697	647	782	304	472	50
LA	124	98	93	107	167	42
CE	239	158	174	188	327	83
ND	83	61	44	62	83	36
SM	11.2	8.7	7.5	8.8	12.0	6.1
EU	1.7	1.4	1.2	1.5	2.3	.4
TB	1.0	.8	.8	.8	.8	.7
YB	4.3	2.9	2.8	3.0	3.4	2.2
LU	1.0	.6	.5	.6	.5	.3
HF	11.1	8.6	8.7	9.5	12.3	4.2
TA	1.43	1.15	1.29	1.12	.95	1.42
PB	45	30	50	15	20	20
TH	28.0	21.8	20.8	21.6	22.3	22.7
U	3.3	3.1	3.6	4.3	3.3	3.7

SAMPLE# FIELD#	61 GU3-17WR	62 GU3-14WR	63 GU3-12	64 GU3-11*	65 GU3-10*	66 GU3-9*
(WT. %)						
SIO2	78.9	78.9	76.6	75.9	76.1	75.5
AL2O3	12.3	12.2	12.7	13.1	13.1	13.4
FE2O3	.97	1.00	.95	.97	.91	1.02
CAO	.45	.48	.51	.54	.55	.55
MGO	.13	.11	.06	.06	.07	.06
TIO2	.09	.10	.09	.09	.09	.09
MNO	.05	.05	.10	.07	.07	.06
NA2O	3.92	4.25	3.51	3.51	3.62	3.78
K2O	3.18	2.94	5.51	5.80	5.50	5.52
P2O5	.01	.03	.01	.01	.01	.01
(PPM)						
BE	3.0	3.1	3.1	3.1	3.1	2.9
SC	2	2	2	2	2	3
V	3	3	2	2	3	3
CR	-	-	-	-	-	-
CO	.2	.2	.2	.2	.2	.2
NI	<1	5	<1	<1	16	<1
CU	2	4	3	5	10	2
ZN	46	50	55	56	57	50
RB	201	187	217	215	197	232
SR	18	18	20	17	22	23
ZR	123	167	122	146	100	181
SB	.4	.4	.7	.4	.3	.4
CS	4.27	4.40	5.48	5.58	5.66	7.17
BA	32	30	160	35	42	67
LA	32	38	30	30	29	29
CE	72	70	65	28	70	81
ND	23	35	26	24	-	30
SM	4.5	5.7	5.3	5.4	5.0	5.2
EU	.3	.3	.2	.2	.2	.3
TB	.6	.7	.7	.7	.7	.8
YB	2.9	2.8	2.9	2.0	3.3	3.4
LU	.5	.5	.6	.5	.3	.6
HF	5.1	5.2	4.6	4.4	4.6	5.4
TA	1.43	1.36	1.35	1.32	1.35	1.53
PB	20	20	30	35	30	25
TH	23.1	23.3	21.7	22.3	21.5	26.0
U	4.4	4.4	4.5	4.4	3.5	4.3

SAMPLE# FIELD#	67 GU3-8*	68 GU3-7*	69 GU3-6*	70 GU3-5*	71 GU3-2*	72 GU3-1*
(WT. %)						
SIO2	76.4	75.8	76.7	77.6	76.3	76.3
AL2O3	13.1	13.3	12.8	12.4	12.8	13.3
FE2O3	1.03	.96	.99	.95	1.00	1.00
CAO	.57	.59	.54	.56	.58	.70
MGO	.09	.11	.06	.08	.06	.09
TIO2	.10	.11	.08	.09	.08	.09
MNO	.10	.12	.07	.09	.06	.09
NA2O	3.52	3.78	3.93	3.67	3.99	4.02
K2O	5.13	5.15	4.84	4.54	5.08	4.47
P2O5	.02	.02	.02	.01	.02	.01
(PPM)						
BE	3.1	3.2	2.9	2.8	2.9	3.1
SC	3	2	2	2	3	2
V	3	3	2	3	<.5	1
CR	-	1	-	-	-	2
CO	.2	.2	.2	0.0	.1	.2
NI	<1	<1	<1	<1	3	11
CU	5	3	2	4	1	6
ZN	77	77	51	64	43	67
RB	241	182	163	203	196	184
SR	34	44	22	31	21	35
ZR	141	147	117	-	136	147
SB	.5	.3	.3	.5	.4	.5
CS	7.89	5.07	5.64	6.24	5.57	6.50
BA	42	42	60	90	47	42
LA	33	32	32	31	31	38
CE	79	71	58	56	72	66
ND	36	30	23	-	29	249
SM	5.9	4.3	5.1	5.5	5.2	5.4
EU	.3	.2	.2	0.0	.2	.2
TB	.9	.6	.6	0.0	.7	.7
YB	3.7	2.7	2.5	2.7	2.6	3.0
LU	.4	.5	.2	0.0	.2	.5
HF	5.9	4.3	4.0	0.0	4.1	4.6
TA	1.60	1.25	1.10	0.00	1.38	1.33
PB	25	30	25	25	20	25
TH	26.1	20.7	19.0	22.0	20.4	22.1
U	5.1	4.8	4.6	5.1	3.8	5.3

FIGURE CAPTIONS

Figure 1: Distribution and thickness of the Topopah Spring Member of the Paintbrush Tuff (Lipman et al., 1966). Locations of measured sections and chemically analyzed samples indicated by two letter ID's as follows: BB = Busted Butte; CP = 311 Wash; LW = Lathrop Wells; GU = USW-GU3 drill hole.

Figure 2: Textural variations among individual pumice lumps within a sample of whole-rock tuff.

Figure 3: Measured sections of the Topopah Spring Member, showing variations in depositional units, welding zones, and crystallization zones (Lipman et al., 1966). Numbers on the right of each section correspond to the sample number of chemically analyzed specimens in table 2.

Figure 4: Variation of major element oxides with stratigraphic height. Analytical data from table 2. Solid symbols = whole pumice; open symbols = whole-rock tuff. (A) Busted Butte; (B) 311 wash; (C) Lathrop Wells; (D) USW-GU3.

Figure 5: Variation of major element oxides vs. silica. Units in weight percent. Solid symbols = whole pumice; open symbols = whole-rock tuff. Source of analytical data: squares - table 2; diamonds - Lipman et al., (1966).

Figure 6: Chondrite-normalized RRE abundances (log scale) vs. atomic number. Solid symbols = whole pumice; open symbols = whole-rock tuff. (A) All samples; (B) quartz latite (low-silica rhyolite); (C) high-silica rhyolite.

Figure 7: Chondrite-normalized RRE patterns in relation to stratigraphic position. Solid symbols = whole pumice; open symbols = whole-rock tuff. (A) Busted Butte; (B) 311 Wash; (C) Lathrop Wells; (D) USW-GU3.

Figure 8: Trace element abundances (ppm) vs. silica (wt. %). Solid symbols = whole pumice; open symbols = whole-rock tuff.

Figure 9: Inter-element variation of selected trace elements (ppm). Solid symbols = whole pumice; open symbols = whole-rock tuff.

Figure 10: Estimated quench temperature and oxygen fugacity determined from coexisting ilmenite and magnetite phenocrysts. MNO, NNO, and FMQ indicate the experimental buffer curves for MnO-Mn₃O₄, nickel-nickel oxide, and fayalite-magnetite-quartz, respectively, at 1 bar total pressure (Haggerty, 1976).

Figure 11: Estimated quench temperature of samples in relation to stratigraphic position in the ash-flow sheet. Solid symbols = whole pumice; open symbols = whole-rock tuff. (A) Lathrop Wells; (B) Busted Butte; (C) 311 Wash; (D) USW-GU3.

Figure 12: Chemical variation with estimated quench temperature. SiO_2 in weight %, all other elements in ppm. Solid symbols = whole pumice; open symbols = whole-rock tuff.

Figure 13: Cross-sectional cartoon of a layered magma body. Circles represent cross-sections through hyperbolic eruption isochrons (Blake, 1981), indicating the locus of points within the magma chamber of magma that will reach the vent simultaneously.

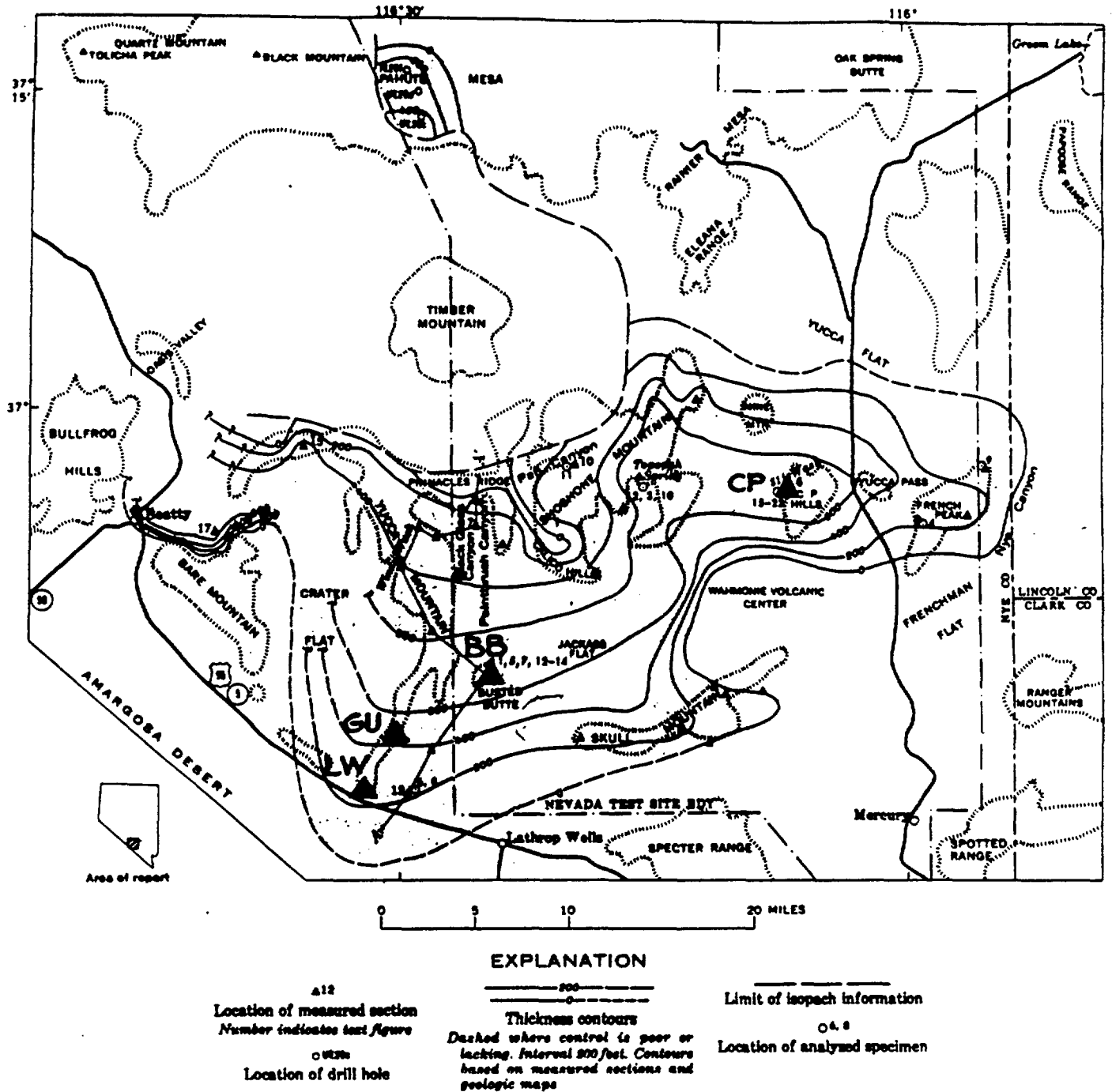


FIGURE 1.—Distribution and thickness of the Topopah Spring Member of the Paintbrush Tuff and location of measured sections and chemically analyzed samples. Section A-A' is shown on plate 1.

Fig. 1



Fig. 2

Fig. 3

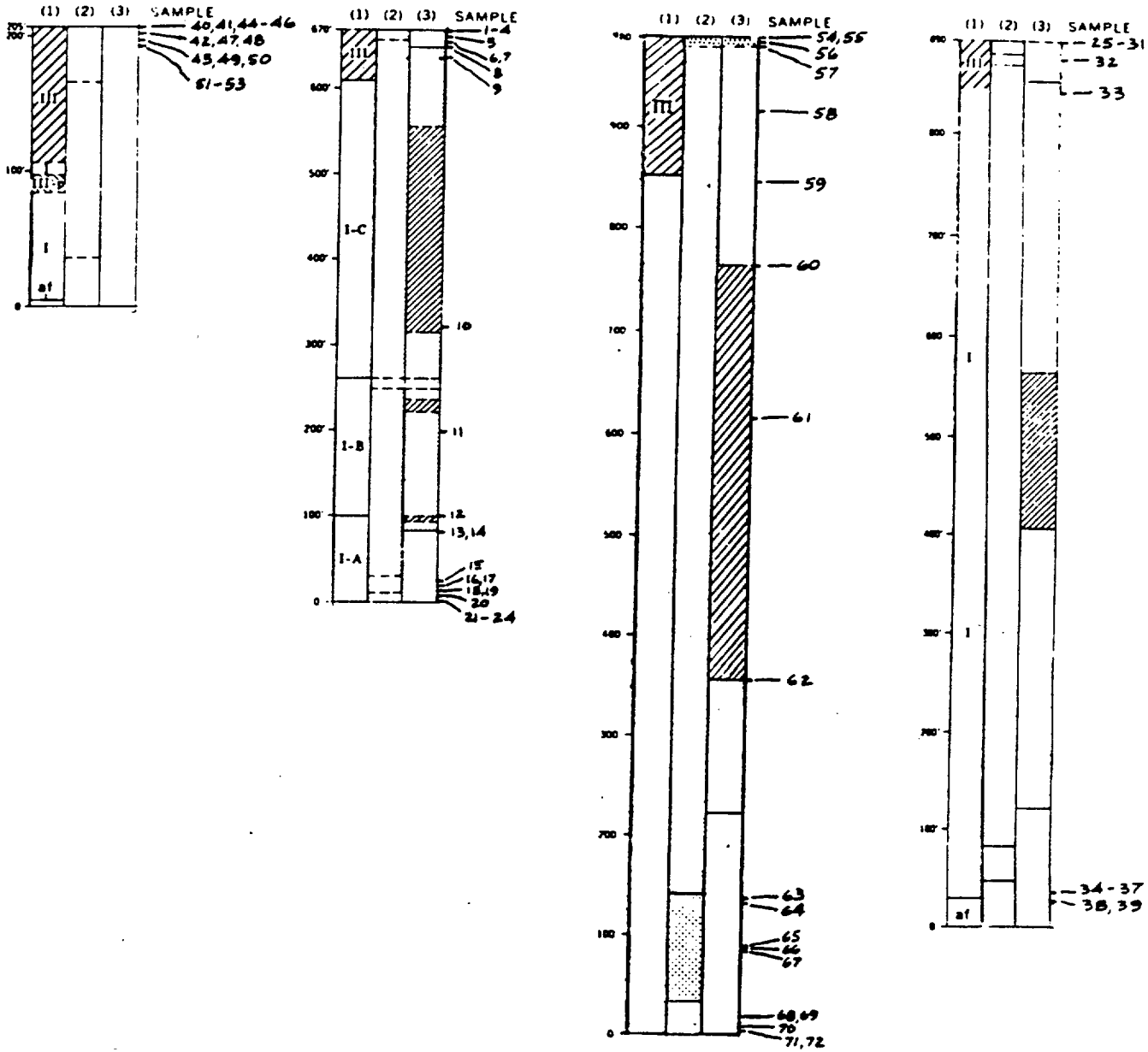
Measured section of the Topopah Spring Member

Lathrop Wells

Husted Butte



USW-GU3

311 Wash



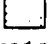



EXPLANATION





(1)
DEPOSITIONAL UNITS

-  Crystal-rich quartz latitic caprock
-  Crystal-poor rhyolite
Locally recognized flow units

(2)
WELDING ZONES

-  Nonwelded
-  Partly welded
-  Nonwelded and partly welded
-  Densely welded

(3)
CRYSTALLIZATION ZONES

-  Glassy
-  Crystalline
-  Vapor phase
-  Lithophysal

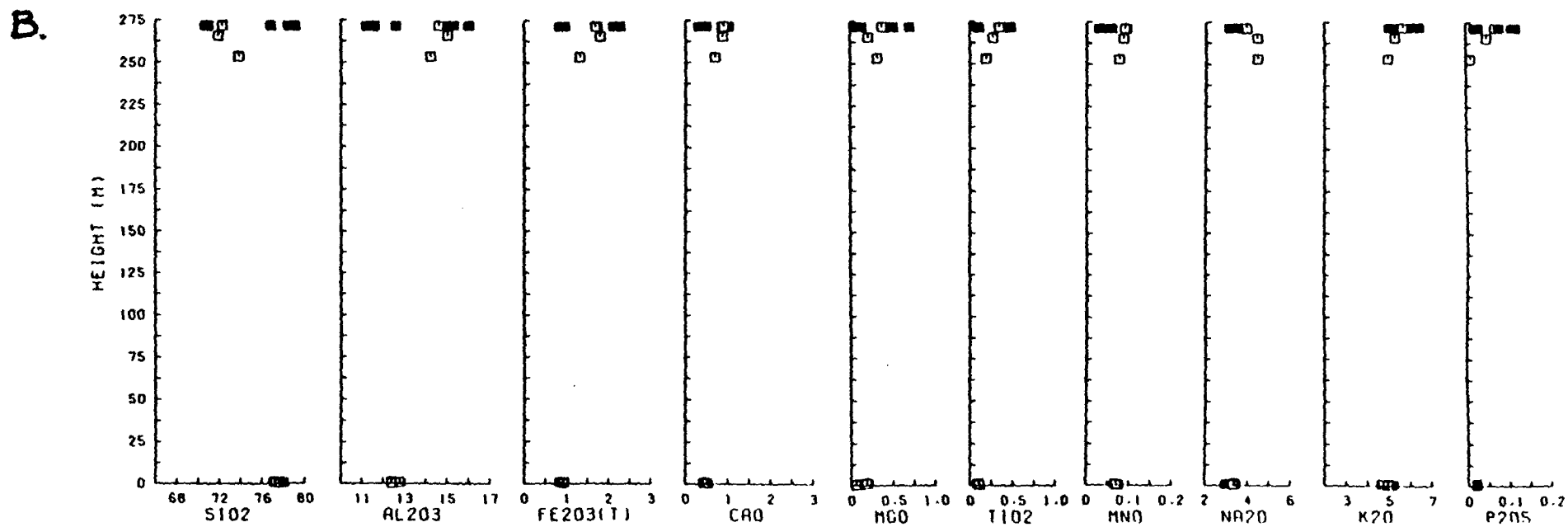
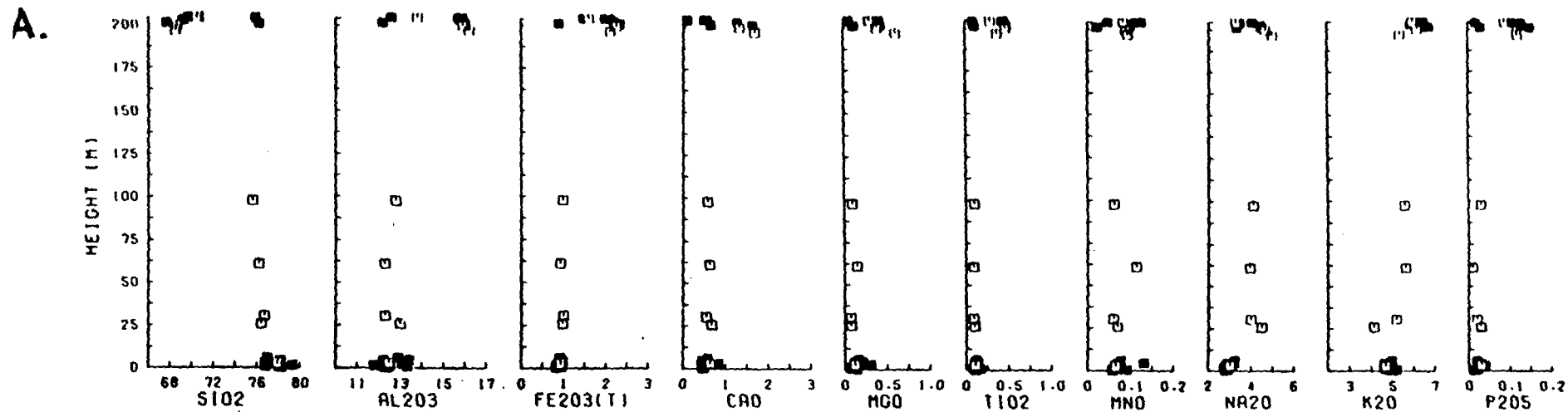
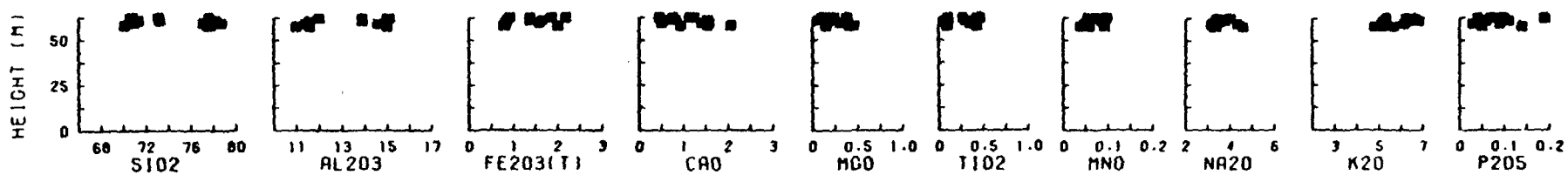


Fig. 4

C.



D.

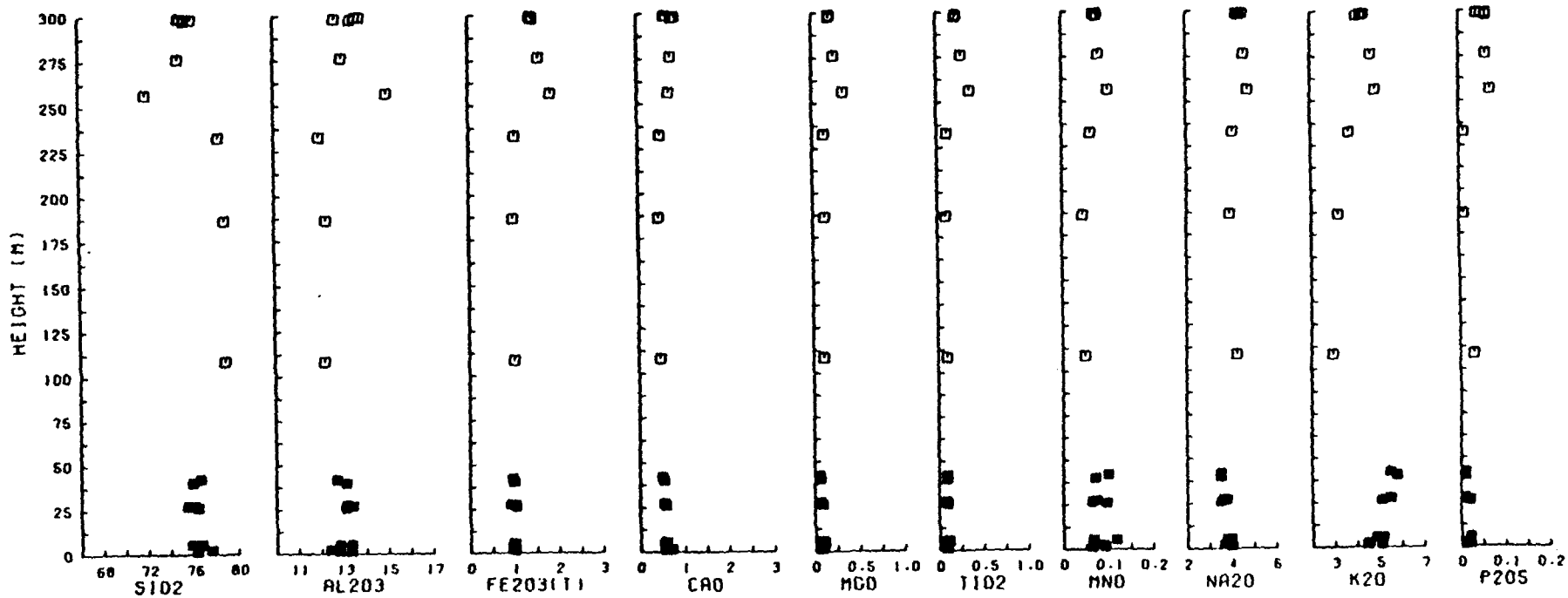


Fig. 4

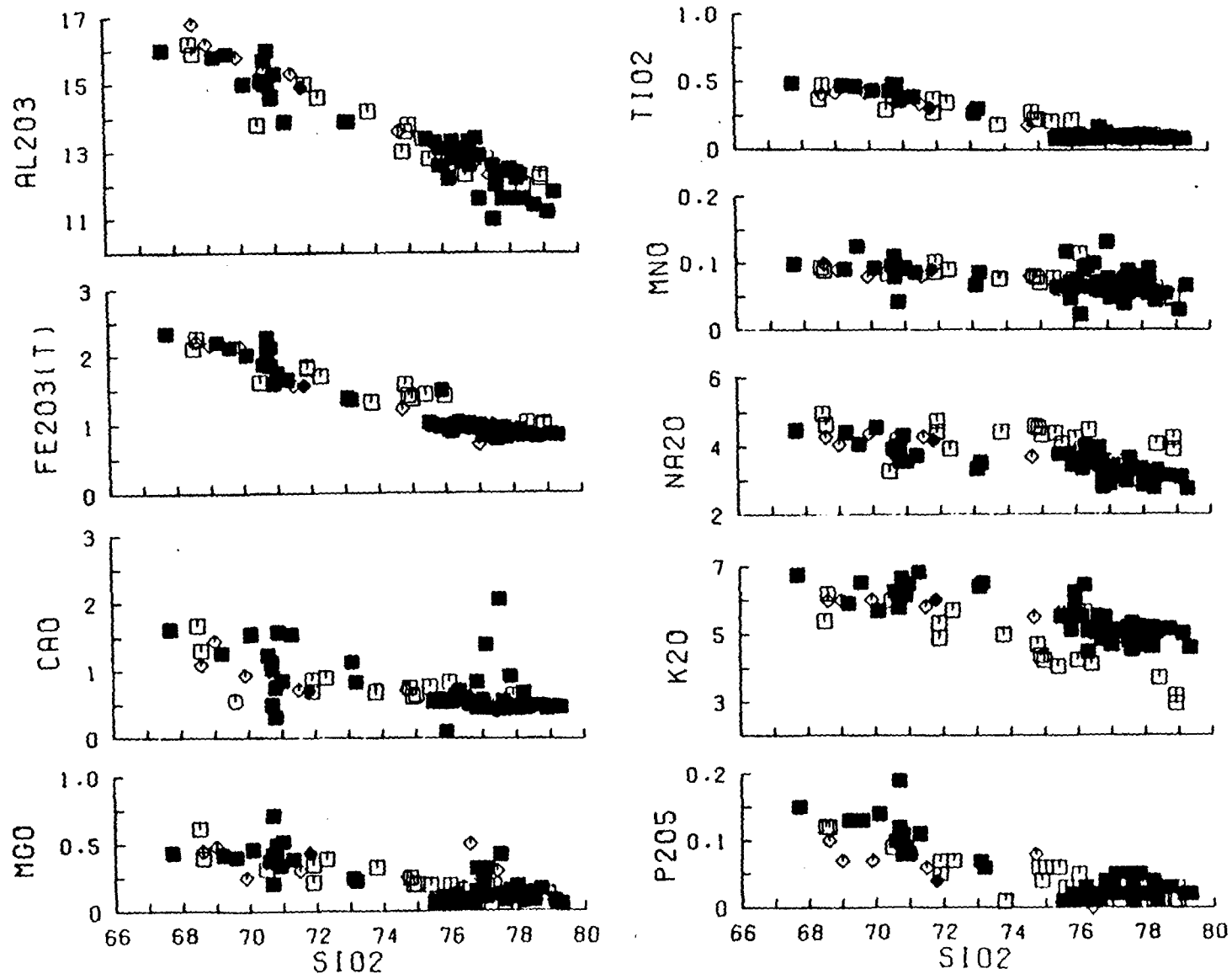


Fig. 5

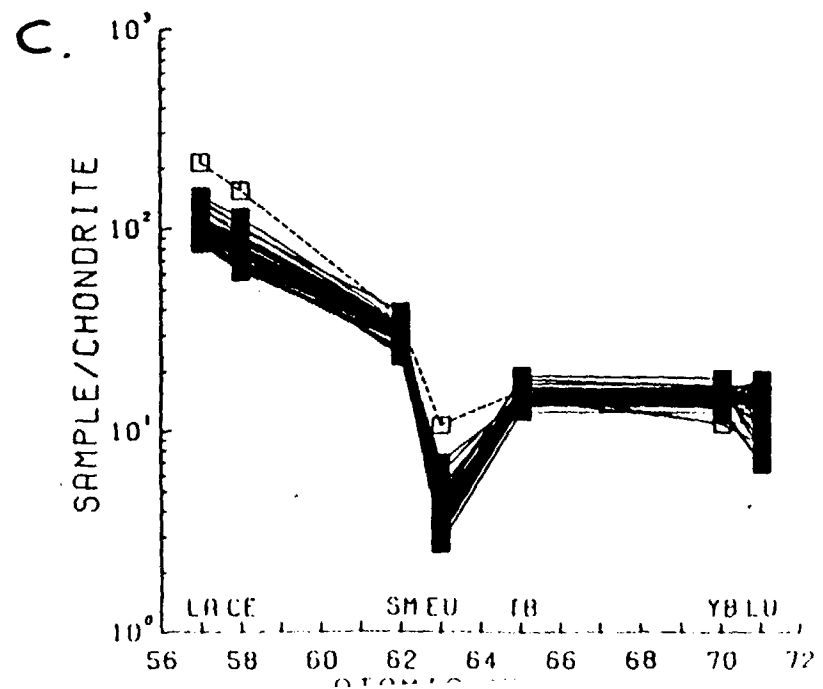
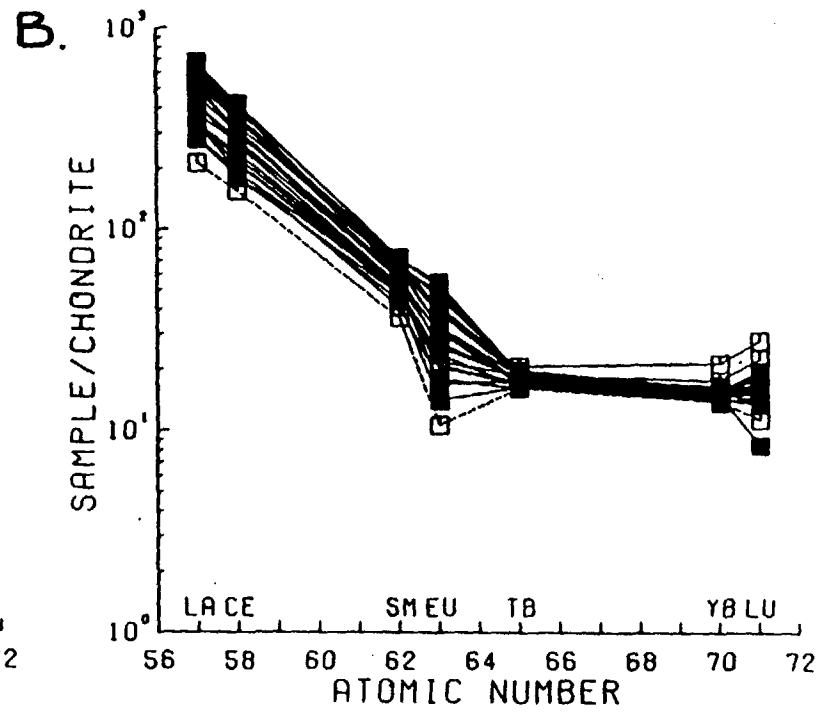
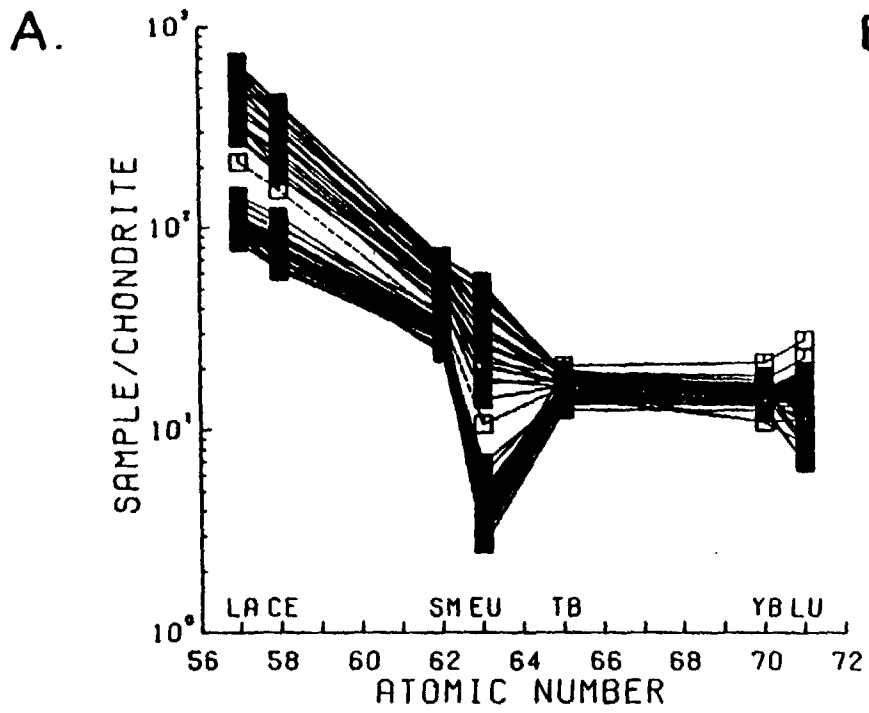
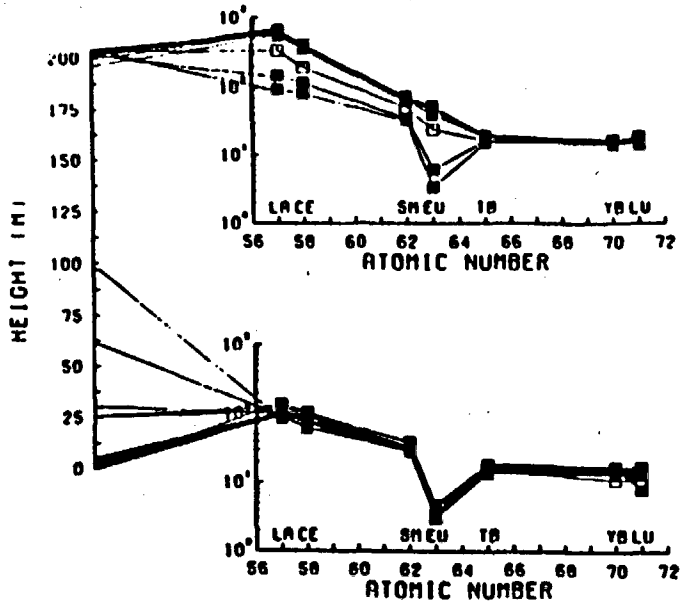
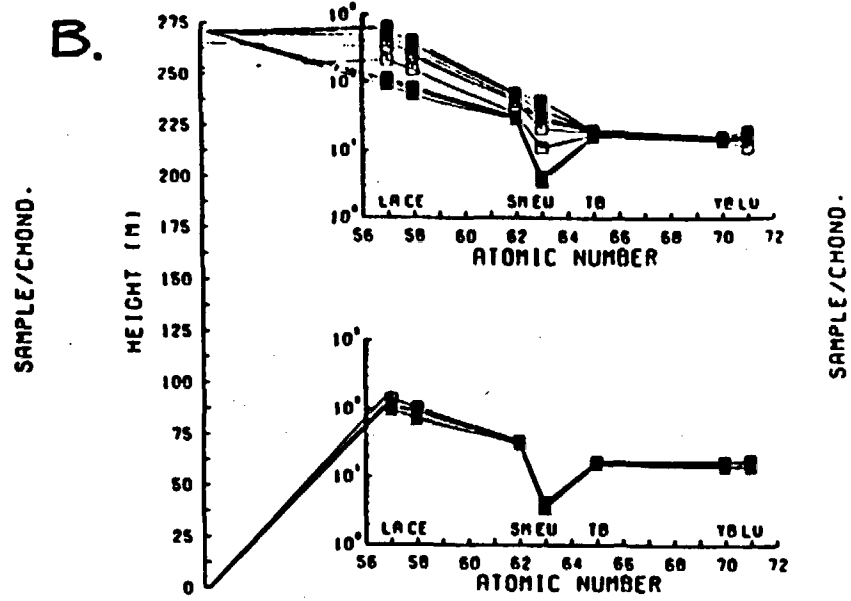


Fig. 6

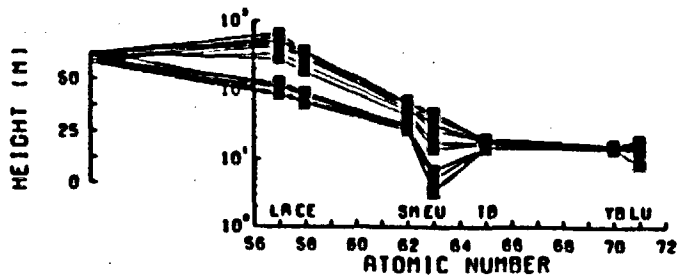
A.



B.



C.



D.

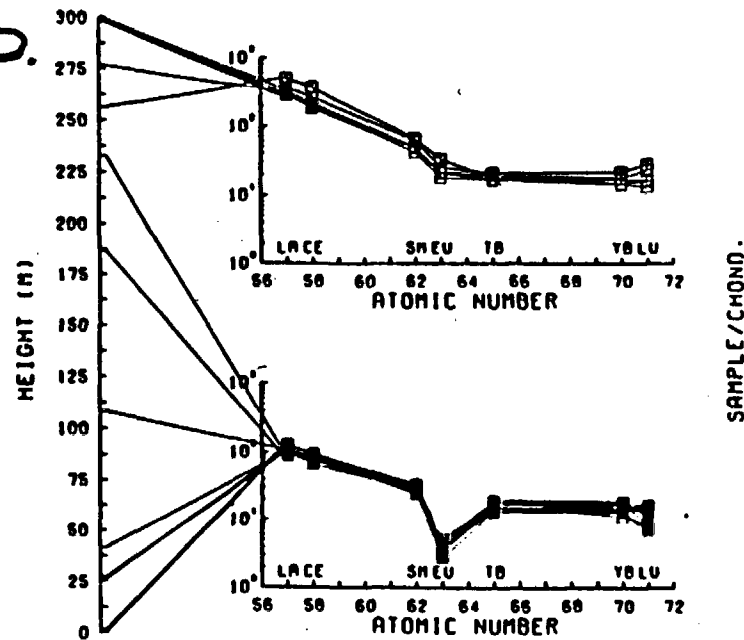


Fig. 7

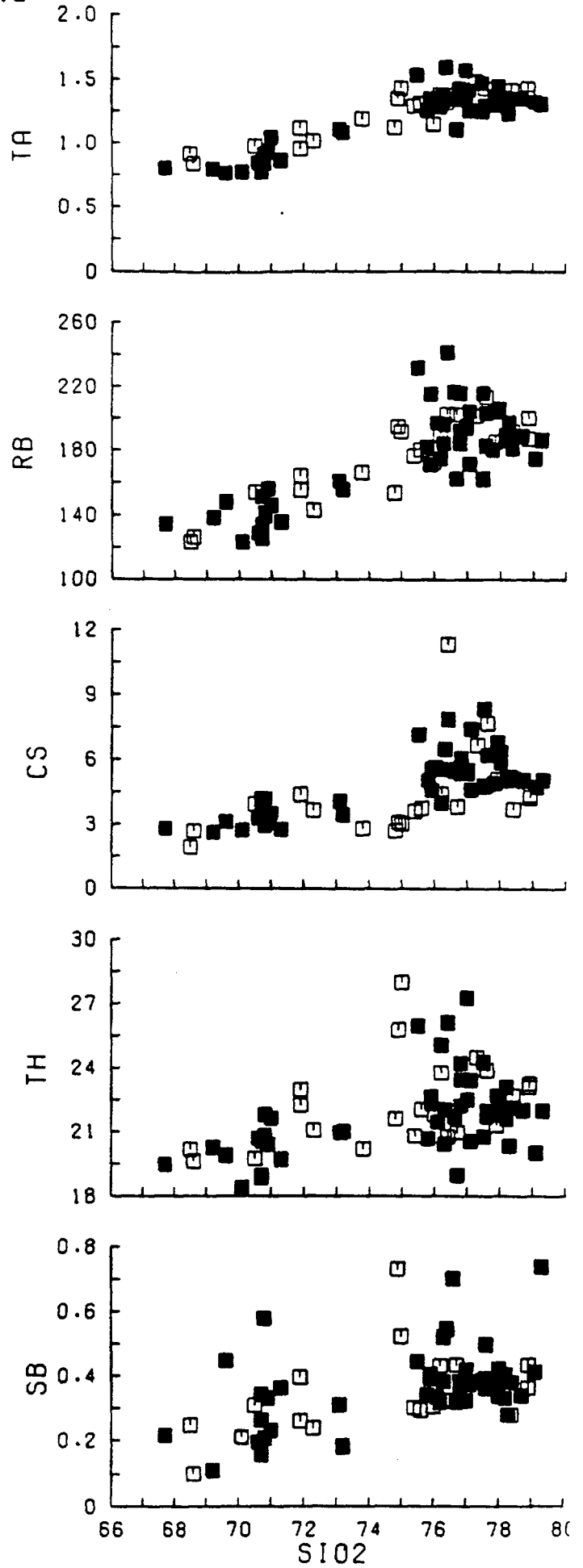
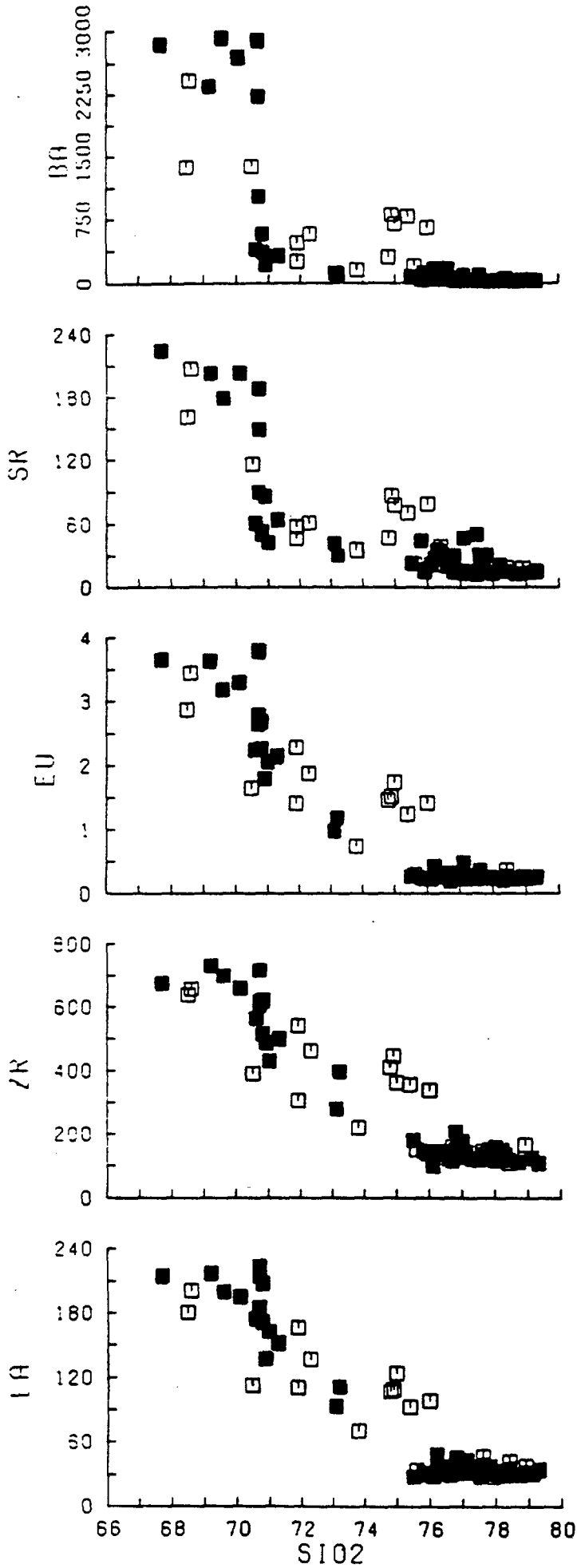
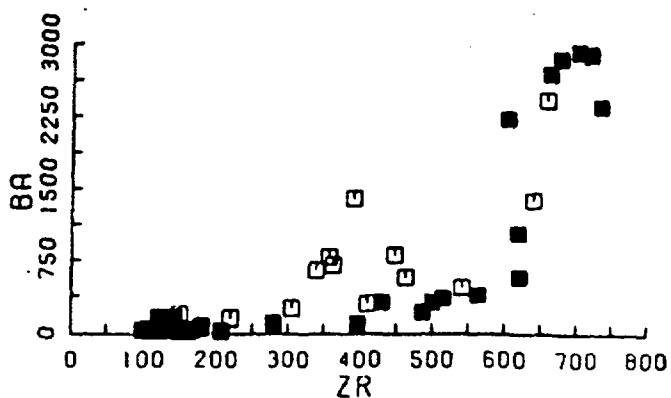
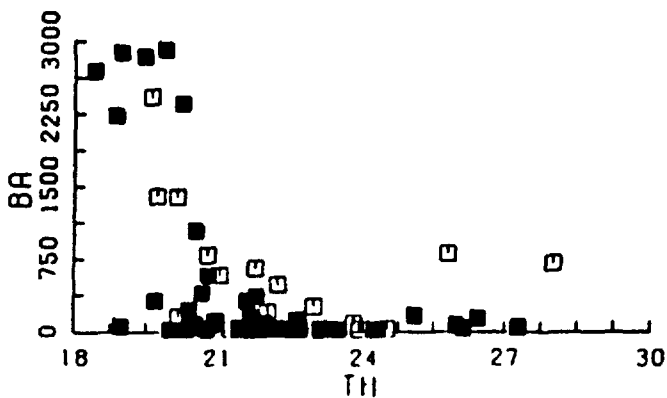
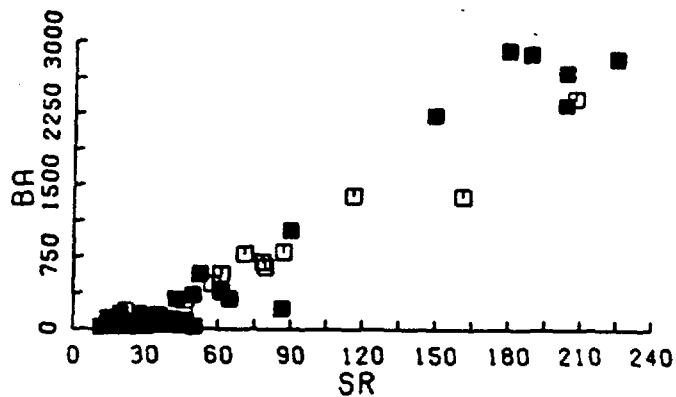
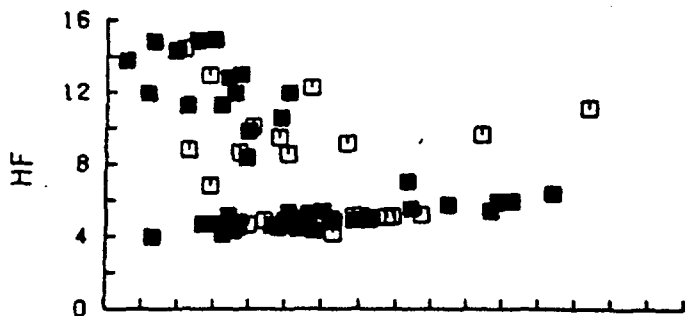
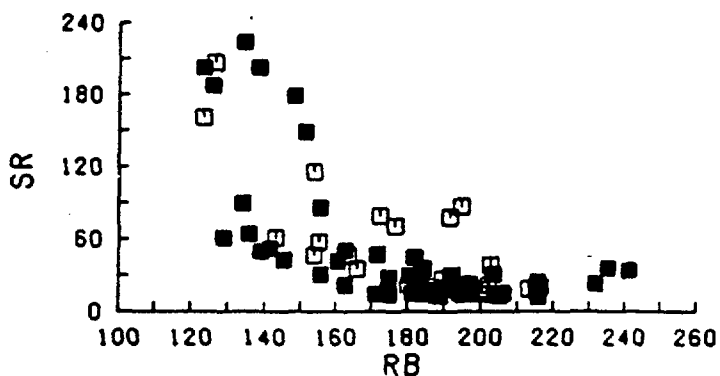
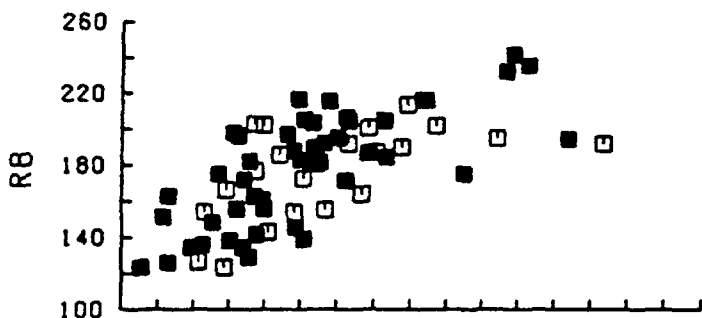
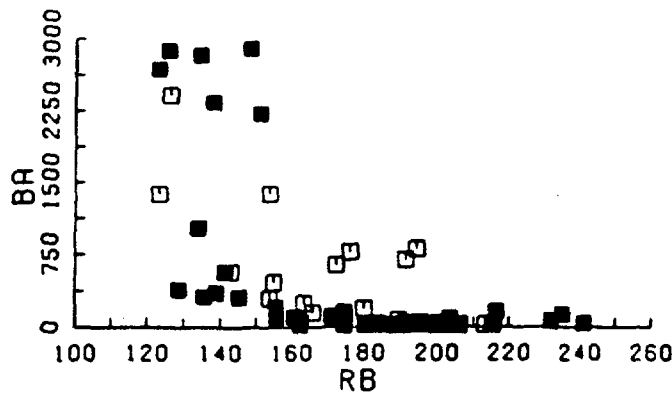
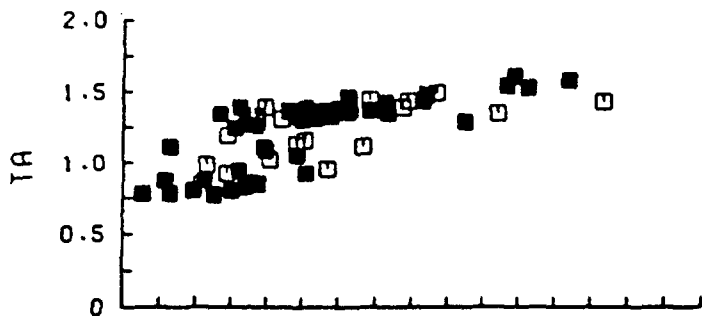


Fig. 9



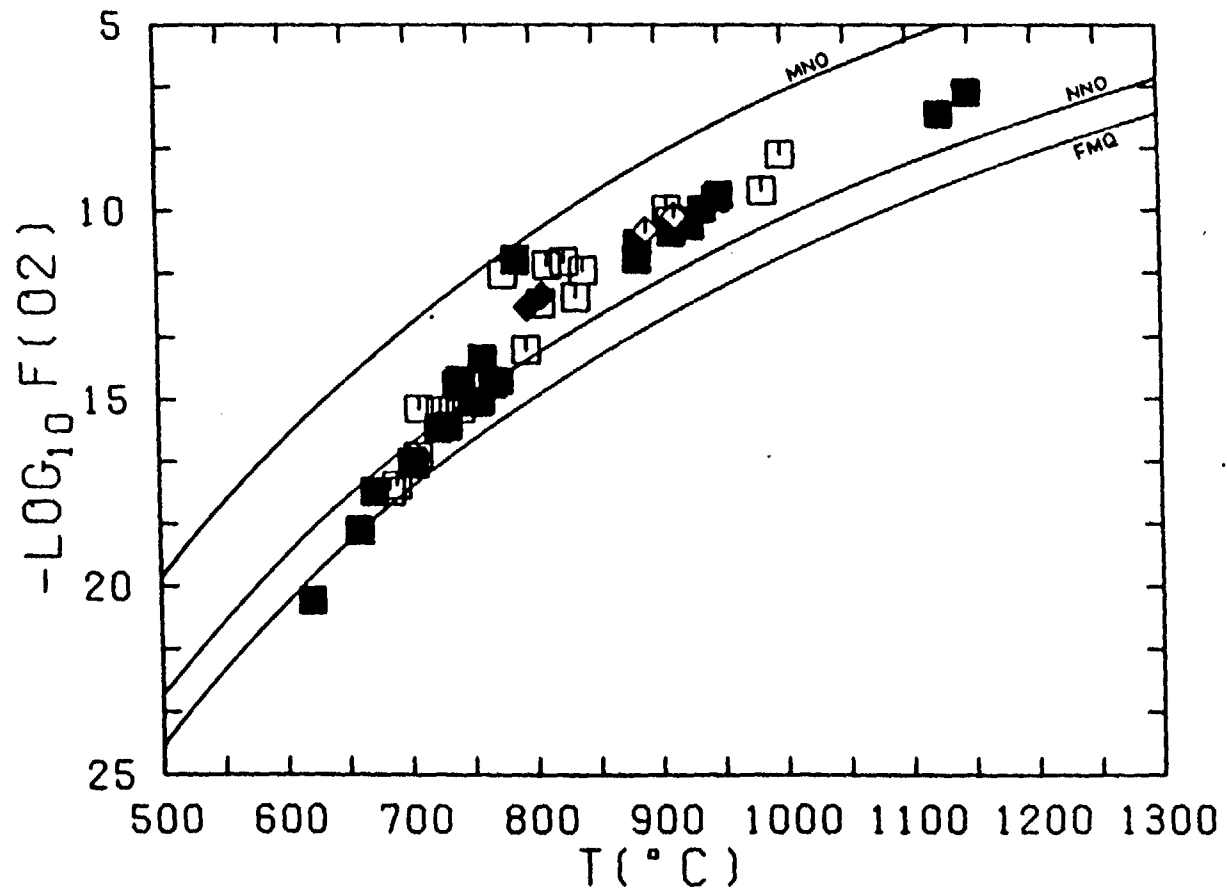


Fig. 10

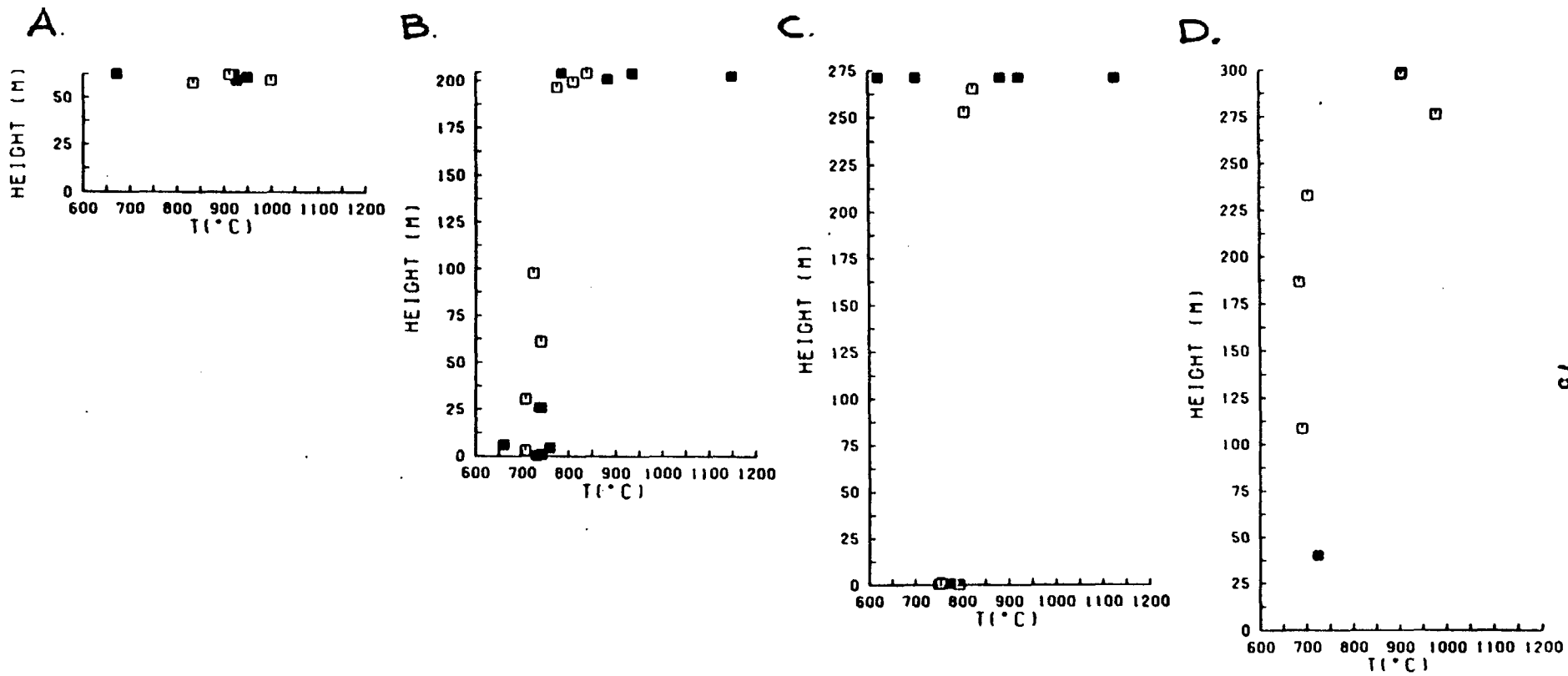


Fig. 11

Fig. 12

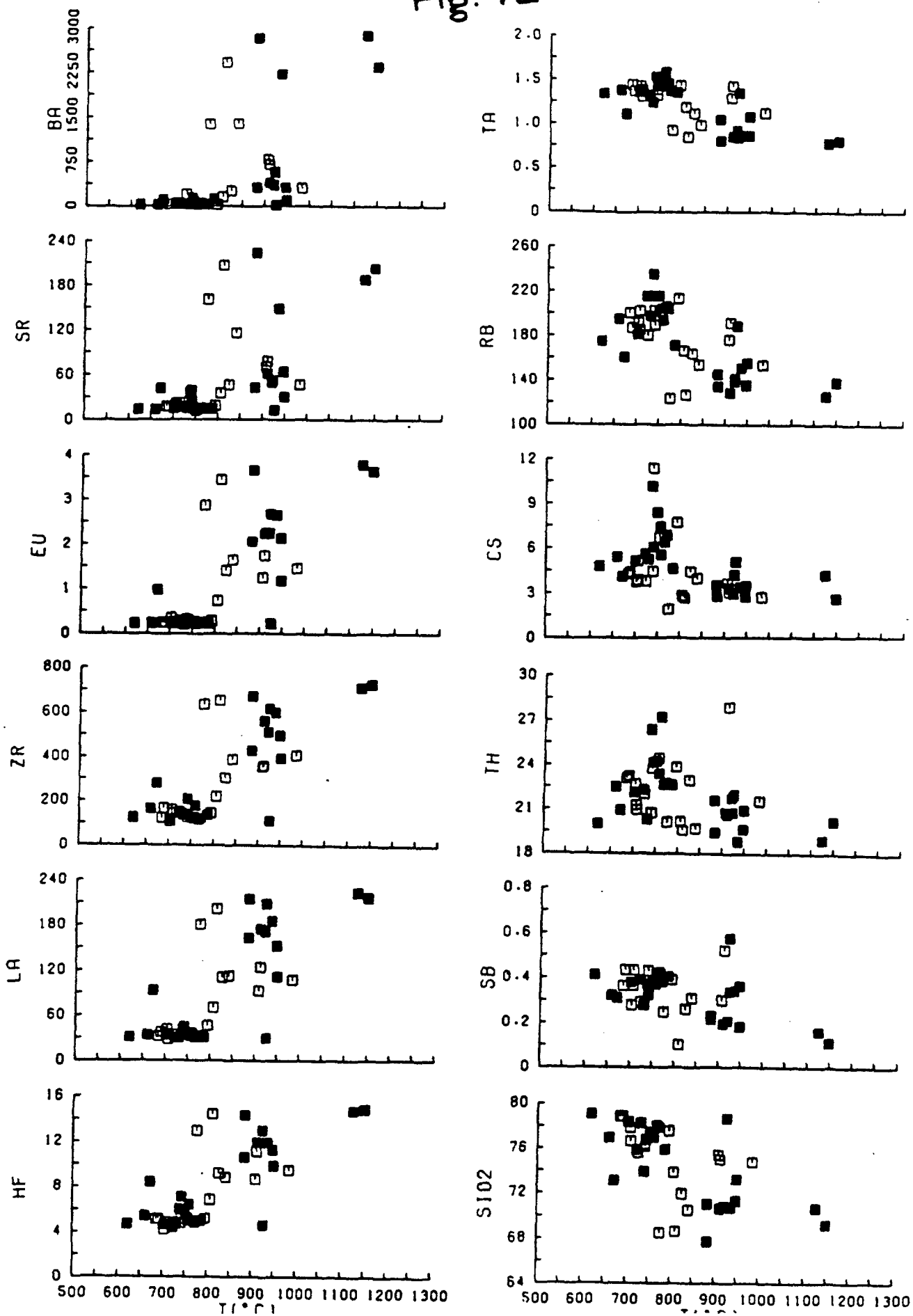
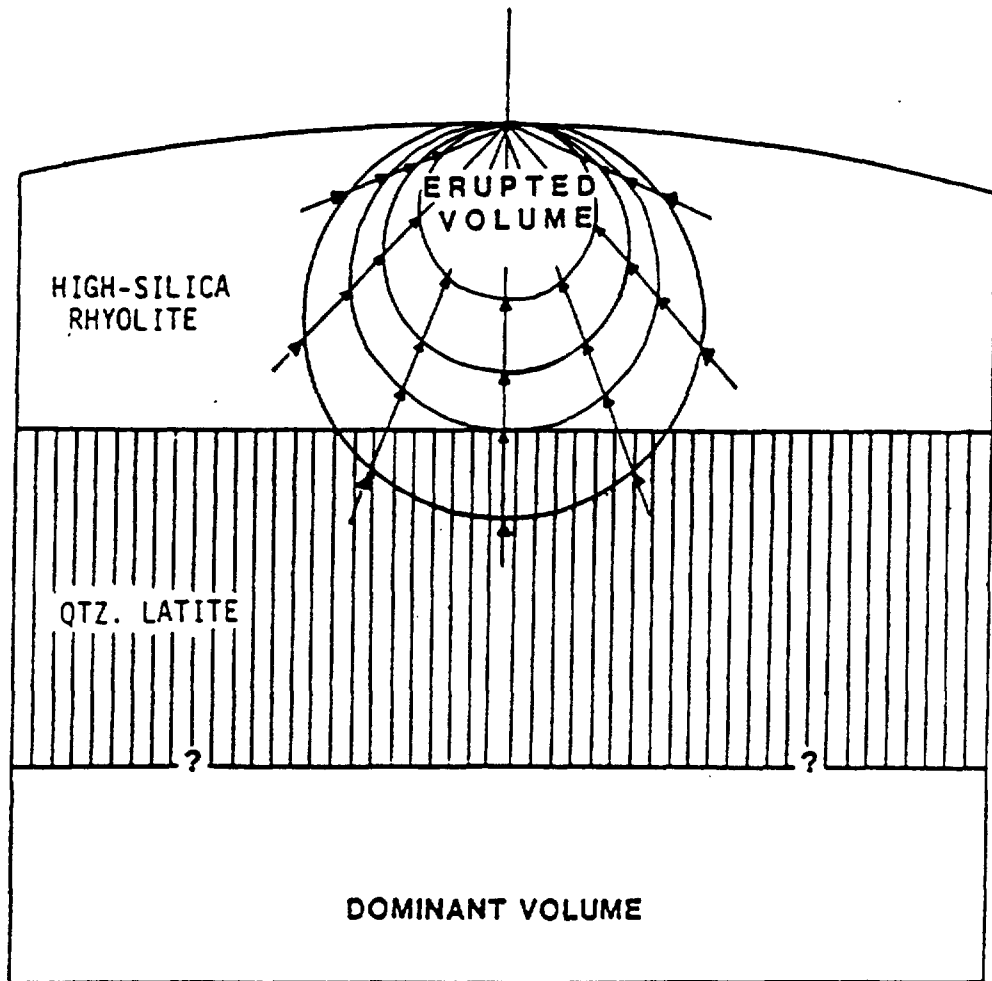


Fig. 13



ERUPTION OF THE TOPOPAH SPRING MEMBER

APPENDIX 1. Microprobe analyses of ilmenite and magnetite phenocrysts and mole fraction of ilmenite (ILM) and ulvospinel (USP) calculated according to the method of Stormer (1983). Asterisks indicate the mean values used for estimated temperature and oxygen fugacity determinations.

SAMPLE ID	TiO ₂	Cr ₂ O ₃	Al ₂ O ₃	Fe ₂ O ₃	FeO	MgO	MnO	TOTAL	USP	I
LW4-10WR	9.37	.02	1.01	48.36	35.29	1.04	2.16	97.25	.264	
	9.57	.04	1.22	47.29	36.51	.47	1.99	97.10	.281	
	7.63	.04	1.09	51.67	34.06	.89	2.08	97.46	.216	
*	8.86	.03	1.11	49.10	35.29	.80	2.08	97.27	.254	
*	36.39	0.00	.22	29.96	24.21	2.95	3.21	96.94		.61
LW4-15WR	3.86	.05	3.12	59.90	19.92	5.16	6.91	98.92	.071	
	10.10	0.00	1.89	46.43	35.07	1.79	2.10	97.37	.287	
	16.91	.03	2.08	31.53	41.96	1.45	1.51	95.47	.519	
*	10.29	.03	2.36	45.95	32.31	2.80	3.51	97.25	.277	
	44.56	0.00	.38	13.48	34.19	2.23	1.88	96.72		.85
	44.64	0.00	.17	12.80	33.64	2.19	2.57	96.00		.86
*	44.60	0.00	.28	13.15	33.91	2.21	2.23	96.38		.86
LW4-1WR	9.84	0.00	1.78	47.18	35.56	1.57	1.80	97.73	.281	
	10.91	.02	3.34	44.86	36.11	2.42	1.72	99.39	.317	
	10.92	0.00	2.68	44.66	36.64	1.95	1.49	98.33	.320	
	7.31	.01	1.76	51.91	31.73	2.19	2.08	96.99	.200	
	8.84	.03	2.07	48.90	34.45	1.77	1.75	97.81	.252	
	9.65	.02	.91	48.16	36.75	.44	2.11	98.05	.276	
	10.13	0.00	1.84	45.46	36.97	.98	1.24	96.62	.305	
	9.32	.03	2.38	48.28	35.10	1.97	1.54	98.62	.267	
	8.04	.03	1.81	50.21	34.25	1.11	2.08	97.53	.232	
	11.02	.06	2.51	43.56	35.51	2.12	1.90	96.67	.322	
*	9.72	.02	2.16	47.08	35.43	1.68	1.75	97.84	.281	
	42.60	0.00	.23	22.81	22.94	6.12	4.40	99.11		.74
	43.89	0.00	.22	15.21	32.92	2.50	2.07	96.80		.84
	42.79	0.00	.23	20.56	24.72	5.36	4.15	97.81		.76
	44.37	0.00	.27	13.66	34.02	2.32	1.72	96.36		.85
*	43.41	0.00	.24	18.08	28.63	4.08	3.09	97.53		.80
LW4-5B	9.39	0.00	1.52	49.08	34.26	1.93	2.31	98.49	.255	
	7.76	0.00	.95	50.44	32.88	1.13	2.39	95.55	.218	
	8.36	0.00	.90	49.31	32.78	1.40	2.55	95.30	.232	
	8.97	0.00	.74	47.81	35.08	.38	2.37	95.35	.261	
*	8.90	0.00	1.28	49.32	33.88	1.59	2.35	97.32	.245	
	36.20	0.00	.18	28.61	27.21	1.68	2.32	96.20		.69
	39.36	0.00	.07	22.62	29.47	1.90	2.51	95.93		.76
	38.92	0.00	.04	22.64	28.94	1.81	2.80	95.15		.75
*	37.67	0.00	.12	25.63	28.20	1.77	2.49	95.88		.72
BB8-10WR	10.75	.02	1.32	43.91	37.32	.37	2.03	95.72	.323	
	9.06	.03	1.10	48.43	35.49	.42	2.60	97.13	.261	
	8.83	.02	1.05	48.60	35.54	.48	2.07	96.59	.258	
*	9.63	.02	1.17	46.80	36.17	.42	2.26	96.47	.283	

	51.17	.03	.02	.62	39.50	1.15	4.41	96.90	.9
	45.57	.05	.06	11.83	33.04	1.39	5.39	97.34	.8
	49.82	.01	.06	1.81	38.27	.94	4.79	95.70	.9
	48.02	.04	.06	6.50	37.55	.59	4.52	97.28	.9
	47.81	.02	.07	7.52	36.14	1.11	4.81	97.48	.9
*	48.15	.03	.06	6.32	36.46	1.08	4.85	96.95	.9
BB8-1									
	10.21	.02	1.09	46.52	36.99	.57	2.04	97.44	.296
	9.79	.03	1.04	46.81	36.17	.69	1.99	96.52	.284
	10.52	.06	.89	45.27	37.30	.43	1.85	96.33	.309
*	10.11	.04	1.00	46.23	36.70	.58	1.95	96.61	.295
	48.52	.02	.07	7.91	35.87	1.18	5.59	99.15	.9
	48.35	.01	.07	6.61	37.32	.66	4.92	97.94	.9
	48.12	.01	.08	8.25	38.00	.93	3.57	98.96	.9
	49.43	.01	.12	4.72	38.98	1.04	3.57	97.87	.9
	47.88	.01	.05	8.91	35.40	1.18	5.48	98.91	.9
*	48.45	.01	.08	7.31	37.32	.98	4.44	98.59	.9
LW4-1B									
	6.83	.01	1.21	52.45	33.09	.82	2.16	96.58	.195
	8.48	.08	1.18	49.74	34.95	.87	1.97	97.27	.243
	6.62	.06	1.36	52.29	32.49	.89	2.31	96.02	.190
	7.13	.03	1.36	52.54	33.38	.87	2.47	97.78	.201
	7.16	.01	1.00	52.14	34.33	.53	1.75	96.91	.208
*	7.24	.04	1.22	51.84	33.64	.80	2.13	96.91	.207
	48.94	.02	.07	6.24	29.98	3.27	8.10	96.62	.92
	48.55	0.00	.09	4.22	38.19	1.39	2.95	95.39	.95
*	48.81	.01	.07	5.55	32.72	2.64	6.38	96.19	.93
BB8-3B									
	7.52	.02	.89	51.34	34.11	.51	2.21	96.60	.216
	7.50	0.00	.88	51.03	33.54	.60	2.43	95.98	.214
*	7.51	.01	.88	51.18	33.83	.55	2.32	96.28	.215
	47.61	.04	.02	6.84	36.18	.51	5.65	96.86	.92
	47.60	.02	.10	8.51	36.23	1.33	4.15	97.94	.91
	45.95	.01	.06	12.20	33.29	.98	6.20	98.69	.87
	47.14	0.00	.07	7.93	35.63	1.16	4.63	96.56	.91
	44.44	0.00	.06	11.68	34.11	.94	4.12	95.35	.87
	47.49	0.00	.03	7.10	35.95	1.22	4.52	96.31	.92
	46.59	0.00	.07	9.88	34.99	1.12	4.85	97.50	.89
	46.57	0.00	.08	11.29	33.23	1.55	5.81	98.53	.88
	45.98	0.00	.05	11.48	33.59	1.20	5.55	97.85	.87
	47.48	0.00	.12	7.92	36.39	.63	5.12	97.65	.91
	46.21	.04	.08	12.45	32.85	1.78	5.46	98.87	.86
	48.63	.02	.09	5.54	37.12	1.19	4.43	97.03	.94
*	46.95	.01	.07	9.38	35.13	1.17	4.94	97.65	.90
CP3-2A									
	12.37	.03	1.01	41.01	39.28	.36	1.49	95.55	.373
	13.77	.06	.65	39.43	40.60	.75	1.04	96.30	.404
	12.33	.04	.75	42.96	38.93	.83	1.62	97.46	.353
	8.85	.02	1.38	48.08	35.19	.51	2.40	96.43	.260
	9.42	.02	1.64	46.47	33.18	1.30	3.47	95.50	.267
*	11.29	.03	1.10	43.51	37.61	.62	1.93	96.09	.333
*	33.74	.05	.17	33.49	24.15	1.36	3.72	96.68	.64

CP3-1D

9.86	.04	1.75	46.80	35.42	1.55	1.83	97.25	.283	
9.74	.02	1.76	46.51	34.84	1.72	1.76	96.35	.280	
9.87	.01	1.84	46.85	35.45	1.62	1.77	97.40	.283	
10.15	.02	1.77	47.23	35.87	1.75	1.75	98.53	.286	
9.76	.02	1.76	46.97	34.81	1.79	1.91	97.02	.277	
9.94	.01	1.72	46.64	35.57	1.53	1.76	97.16	.286	
9.56	.02	1.74	46.95	34.82	1.65	1.77	96.50	.275	
10.00	.04	1.78	46.20	35.41	1.63	1.71	96.77	.289	
* 9.85	.02	1.76	46.77	35.26	1.65	1.78	97.09	.282	
41.59	.02	.21	19.30	31.35	2.30	1.93	96.69		.79
45.07	.01	.19	13.73	32.42	3.18	2.41	97.01		.85
43.04	.04	.16	16.14	32.38	2.48	1.88	96.12		.83
44.48	0.00	.19	13.22	33.16	2.62	2.14	95.82		.86
42.51	.03	.18	17.22	31.37	2.58	2.23	96.11		.81
43.27	.02	.18	16.26	32.00	2.69	2.09	96.51		.82
43.13	.02	.25	15.52	32.17	2.56	2.03	95.68		.83
41.53	.03	.23	19.10	30.48	2.64	2.13	96.14		.79
* 43.14	.02	.20	16.15	31.96	2.64	2.10	96.21		.82

BB8-15B

7.59	.01	1.02	52.61	34.31	.71	2.44	98.69	.211	
6.85	0.00	.85	53.92	32.67	.83	2.99	98.11	.186	
7.01	.02	.84	52.78	32.46	.71	3.19	97.01	.193	
7.31	.01	.94	53.38	33.33	.72	3.18	98.87	.199	
7.32	.02	.98	52.75	33.06	.72	3.21	98.07	.201	
7.12	.02	1.01	52.93	33.58	.73	2.43	97.81	.199	
7.77	0.00	.97	52.26	34.32	.71	2.55	98.59	.216	
7.43	.04	.93	52.77	33.83	.71	2.65	98.36	.206	
* 7.33	.01	.96	52.91	33.59	.73	2.74	98.27	.203	
48.38	.01	.05	5.51	37.97	.95	3.79	96.66		.94
47.47	.01	.05	7.43	34.50	1.33	5.74	96.53		.92
46.80	0.00	.05	11.52	34.84	1.35	4.78	99.33		.88
47.91	0.00	.03	7.13	35.31	.63	6.57	97.57		.92
49.61	0.00	0.00	1.23	43.06	0.00	1.53	95.43		.98
46.43	0.00	.07	13.44	33.29	1.26	6.14	100.63		.86
46.27	0.00	.07	13.42	32.75	1.52	6.07	100.11		.85
45.10	.02	.05	15.58	28.68	1.82	8.52	99.77		.83
45.10	.04	.09	14.46	30.56	1.24	7.69	99.18		.84
44.61	.03	.04	14.51	31.52	1.38	6.06	98.14		.84
* 46.64	.01	.05	10.99	33.96	1.25	5.68	98.58		.88

BB8-20

7.67	.01	1.14	50.79	34.53	.54	1.94	96.62	.224	
9.62	.02	1.10	48.19	36.85	.43	2.12	98.33	.277	
11.20	0.00	1.00	42.86	38.57	0.00	1.54	95.16	.342	
11.28	.02	1.18	43.16	38.45	0.00	2.07	96.15	.341	
* 9.76	.01	1.12	46.73	36.88	.28	1.97	96.75	.289	
47.46	.06	.03	9.45	35.77	.62	5.73	99.12		.90
49.66	.05	.09	1.38	39.13	.76	4.12	95.19		.98
48.60	.05	.07	7.30	35.58	1.05	6.17	98.82		.92
49.66	.04	.14	3.72	38.39	1.03	4.37	97.35		.96
49.79	.04	.08	3.93	39.26	.88	3.90	97.87		.96
* 49.27	.05	.09	4.83	37.91	.92	4.70	97.76		.95

CP1-AFB

10.51	.01	1.14	44.51	37.10	.38	1.93	95.58	.314	
9.54	0.00	1.12	46.08	35.67	.51	2.07	95.00	.284	
* 10.03	.01	1.13	45.30	36.39	.45	2.00	95.31	.299	
47.61	.02	.07	8.07	37.46	.98	3.56	97.77		.9
47.69	.03	.06	8.71	37.55	.99	3.53	98.55		.9
47.35	.01	.06	8.62	37.15	1.01	3.58	97.78		.9
47.44	.03	.06	7.82	37.55	.96	3.36	97.21		.9
46.62	0.00	.07	8.86	36.84	.91	3.42	96.72		.9
47.62	0.00	.09	8.78	37.56	.99	3.45	98.49		.9
47.99	.04	.09	7.73	37.82	.99	3.53	98.18		.9
47.71	.01	.08	8.16	37.65	1.02	3.39	98.02		.9
47.72	.02	.07	7.89	37.71	.96	3.45	97.82		.9
48.50	0.00	.06	6.45	38.95	.81	3.18	97.95		.9
* 47.65	.02	.07	8.11	37.62	.97	3.46	97.89		.9

CP1-AFWR

9.55	.03	1.31	47.81	36.48	.30	2.57	98.05	.277	
10.67	.02	1.31	45.84	35.90	.59	3.75	98.07	.300	
11.14	.03	1.23	43.36	36.52	.24	3.43	95.95	.327	
10.58	.02	1.29	44.53	36.36	.30	3.05	96.13	.311	
10.69	.03	1.35	43.98	37.49	.39	1.77	95.70	.323	
10.92	.02	.44	44.37	36.19	.06	3.58	95.58	.312	
10.65	.02	1.27	45.48	37.62	.36	2.23	97.63	.312	
* 10.48	.02	1.21	45.45	36.76	.34	2.76	97.01	.305	
48.17	.03	.09	8.64	34.65	.99	6.81	99.39		.90
47.58	.02	.09	11.04	36.57	1.00	4.38	100.68		.88
44.66	.01	.13	16.21	32.73	1.59	4.54	99.86		.83
48.64	.01	.09	8.85	38.73	.91	3.34	100.58		.91
47.04	.02	.09	10.15	36.76	.98	3.75	98.79		.89
47.81	.03	.16	9.98	37.17	1.03	3.94	100.12		.89
48.59	.03	.13	8.87	35.43	1.02	6.36	100.44		.90
48.46	.01	.08	8.17	38.77	.87	3.22	99.58		.91
* 47.66	.02	.11	10.17	36.33	1.04	4.62	99.95		.89

LW1-A

9.72	.03	1.90	46.74	35.32	1.57	1.72	97.00	.282	
10.06	.05	1.78	45.41	35.97	1.37	1.37	96.01	.298	
9.41	.05	1.97	47.35	35.75	1.38	1.41	97.31	.276	
9.56	.01	1.92	47.23	34.47	1.91	1.90	97.00	.272	
7.77	.02	1.14	49.87	33.70	.91	1.88	95.29	.226	
8.52	.04	1.99	48.46	34.06	1.52	1.76	96.35	.249	
9.14	.03	1.69	47.20	35.49	1.10	1.41	96.06	.272	
* 9.32	.03	1.85	47.25	35.08	1.46	1.63	96.62	.272	
39.48	0.00	.22	22.18	29.16	2.55	1.77	95.36		.76
44.35	0.00	.16	13.33	34.50	2.04	1.72	96.11		.86
41.95	0.00	.24	18.63	30.87	2.54	2.30	96.53		.80
36.79	0.00	.22	29.25	26.29	2.67	2.01	97.23		.69
36.65	0.00	.15	28.65	26.00	2.46	2.54	96.45		.69
41.74	0.00	.19	19.59	30.19	3.03	1.92	96.66		.79
45.44	0.00	.19	12.43	34.20	2.59	2.02	96.87		.87
42.90	.02	.56	16.21	31.18	3.10	1.85	95.81		.82
41.61	0.00	.21	19.14	29.55	3.21	2.12	95.84		.79
43.03	.01	.24	17.94	27.93	3.99	3.61	96.75		.80

	*	41.72	0.00	.24	19.16	30.10	2.89	2.24	96.35		.791
CP3-2B		8.95	0.00	2.16	47.97	34.06	1.88	1.77	96.79		.258
		10.07	0.00	2.10	45.46	34.89	1.88	1.78	96.17		.293
		9.67	0.00	1.85	46.77	35.11	1.64	1.68	96.72		.279
		9.05	0.00	1.95	47.46	34.63	1.68	1.36	96.13		.265
		9.10	.01	2.24	47.89	33.76	2.18	1.83	97.01		.258
		11.04	0.00	2.00	43.84	36.66	1.55	1.54	96.63		.325
		8.75	0.00	2.42	48.08	33.69	1.97	1.85	96.76		.253
	*	9.49	0.00	2.10	46.84	34.65	1.83	1.69	96.59		.275
		41.82	0.00	.33	18.30	30.82	2.86	1.67	95.79		.805
		41.92	0.00	.32	19.22	30.08	3.36	1.61	96.51		.796
		41.38	.04	.38	20.36	30.45	2.96	1.47	97.04		.786
		38.37	0.00	.35	24.99	27.85	2.88	1.50	95.94		.734
		42.51	0.00	.31	17.28	31.19	3.01	1.65	95.95		.816
		37.82	.02	.31	27.53	26.55	3.32	1.52	97.07		.708
	*	41.17	0.00	.33	20.03	30.00	3.03	1.60	96.16		.787
CP3-1A		10.62	0.00	1.17	44.36	37.81	.27	1.57	95.81		.321
		10.88	0.00	1.03	43.88	37.75	.31	1.71	95.57		.326
		8.11	0.00	.80	50.10	35.61	.20	1.70	96.52		.239
		12.02	0.00	.98	42.18	38.61	.33	2.06	96.19		.356
		10.88	.01	.98	44.03	37.87	.31	1.63	95.71		.326
		7.49	0.00	1.00	50.83	34.80	.35	1.60	96.06		.222
		9.89	0.00	.94	46.44	36.53	.49	1.91	96.20		.290
		6.49	0.00	.77	53.35	34.49	.28	1.21	96.60		.191
	*	9.26	0.00	.96	47.43	36.47	.32	1.61	96.04		.275
		50.79	0.00	.14	2.17	39.24	1.53	3.66	97.53		.977
		47.63	0.00	.07	9.06	37.89	1.03	3.07	98.75		.908
		47.61	0.00	.30	5.52	38.82	.78	2.57	95.60		.943
		49.65	.01	.08	2.32	41.24	.78	1.99	96.07		.976
		39.63	0.00	.15	23.35	29.92	1.11	3.69	97.85		.757
		50.28	0.00	.15	.83	38.65	1.01	4.70	95.62		.991
	*	47.85	0.00	.16	6.39	38.23	.97	3.03	96.63		.934
CP3-1B		9.92	.01	1.08	46.69	37.28	.37	1.65	97.00		.293
		11.53	.01	1.19	43.70	38.10	.70	1.87	97.10		.337
		8.80	.01	1.26	47.94	35.74	.45	1.72	95.92		.263
		10.70	.01	1.17	45.87	38.34	.40	1.64	98.13		.314
		10.15	.01	1.14	45.33	37.06	.40	1.66	95.75		.304
		11.28	0.00	1.29	44.07	38.63	.38	1.69	97.35		.335
		12.44	0.00	1.29	40.68	39.27	.36	1.65	95.70		.377
		10.94	.13	1.33	43.99	38.08	.41	1.63	96.51		.330
		10.97	0.00	1.53	44.62	38.69	.33	1.58	97.72		.329
	*	10.72	.02	1.25	44.90	37.90	.43	1.68	96.90		.319
		48.65	.01	.18	5.21	39.21	.96	2.79	97.01		.946
		50.05	.01	.23	3.05	40.87	.80	2.68	97.69		.969
		50.01	0.00	.16	1.84	40.87	.89	2.48	96.25		.981
		49.71	.02	.19	3.34	41.75	.46	2.10	97.57		.966
	*	49.39	.01	.18	3.68	40.28	.85	2.59	96.98		.962
CP1-3WR		10.05	0.00	1.17	48.01	37.70	.45	1.97	99.35		.288

	11.35	0.00	1.30	44.27	38.00	.79	1.82	97.53	.331	
	11.45	0.00	1.26	44.16	37.76	.79	2.15	97.57	.331	
	11.20	0.00	1.30	44.56	38.65	.41	1.70	97.82	.331	
	10.70	0.00	1.32	44.86	37.84	.40	1.78	96.91	.319	
	11.10	0.00	1.22	43.72	38.01	.42	1.71	96.18	.332	
	12.56	0.00	1.32	43.14	38.62	.32	3.69	99.65	.354	
	10.53	.01	1.22	47.08	38.26	.35	2.07	99.52	.303	
*	11.17	0.00	1.26	44.81	38.09	.51	2.11	97.95	.325	
	48.96	.01	.08	6.93	35.47	.70	7.22	99.36		.92
	49.13	.02	.04	8.48	37.95	1.23	3.99	100.84		.91
	49.29	.02	.07	7.49	38.58	.80	4.26	100.51		.92
	48.79	.03	.08	8.10	38.59	.89	3.65	100.13		.91
	49.71	.02	.07	8.18	38.92	1.17	3.65	101.72		.91
	49.17	0.00	.16	8.66	39.04	.86	3.60	101.49		.91
	49.91	0.00	.08	7.37	40.22	.78	3.23	101.59		.92
	49.04	0.00	.05	8.53	38.42	.82	4.16	101.02		.91
	49.03	0.00	.10	8.45	38.56	1.36	3.07	100.57		.91
*	49.24	.01	.08	7.99	38.40	.95	4.13	100.80		.92
LW2-A										
	8.49	0.00	1.25	48.84	34.54	1.14	1.53	95.79	.247	
	8.89	.01	1.71	48.83	34.32	1.63	1.92	97.30	.252	
	8.89	0.00	1.55	49.77	34.98	1.48	1.83	98.50	.249	
	10.28	0.00	1.47	45.78	35.95	1.60	1.30	96.39	.297	
	9.09	0.00	1.63	48.89	34.64	1.63	1.92	97.81	.255	
	8.91	0.00	1.62	48.67	34.24	1.55	2.03	97.03	.252	
	9.95	.01	1.67	46.31	35.33	1.51	1.86	96.64	.287	
	10.88	.02	1.36	45.69	36.90	1.39	1.69	97.93	.309	
*	9.44	0.00	1.55	47.84	35.11	1.51	1.77	97.22	.269	
	41.22	0.00	.16	19.88	30.61	2.58	1.83	96.28		.79
	42.99	.01	.17	17.11	32.42	2.55	1.67	96.92		.82
	39.30	.02	.22	24.02	29.07	2.41	1.95	96.99		.74
	43.46	.01	.38	15.66	32.87	2.51	1.72	96.61		.83
	36.35	.01	.17	30.38	25.15	2.96	2.23	97.25		.67
	42.83	.02	.20	17.00	32.32	2.53	1.66	96.56		.82
	42.37	.01	.19	18.11	31.57	2.69	1.71	96.65		.81
	41.97	.02	.16	20.21	30.62	2.98	1.79	97.74		.78
	39.33	.03	.58	24.62	29.14	2.42	1.89	98.01		.74
*	41.14	.01	.24	20.59	30.47	2.62	1.83	96.90		.78
LW2-5										
	10.53	0.00	.35	45.55	36.88	.25	2.32	95.88	.303	
	9.68	0.00	1.59	48.31	34.80	2.15	1.61	98.14	.267	
	7.48	0.00	1.62	52.04	32.88	1.61	2.23	97.85	.207	
	7.80	.01	1.57	51.02	32.15	1.84	2.63	97.02	.213	
	9.95	0.00	.95	47.10	35.31	1.28	2.14	96.73	.279	
	7.68	0.00	1.69	50.60	32.38	1.68	2.36	96.39	.215	
	9.19	.01	1.60	48.33	34.67	1.79	1.52	97.11	.260	
*	8.71	0.00	1.46	49.38	33.83	1.66	2.09	97.13	.243	
	36.75	.01	.32	30.49	26.19	2.68	2.05	98.50		.68
	40.30	.02	.20	22.24	29.89	2.01	2.73	97.39		.76
	36.99	.01	.26	29.64	25.95	2.76	2.36	97.97		.68
	50.40	.01	.14	1.93	40.47	1.29	2.52	96.76		.98
	36.67	.01	.49	30.06	26.30	2.51	2.17	98.21		.68

	36.59	0.00	.22	30.72	25.92	2.62	2.28	98.36	.67
	37.82	.01	.25	28.17	26.96	2.60	2.38	98.19	.70
*	38.54	.01	.28	26.45	27.94	2.44	2.34	98.00	.72
LW2-10									
	10.96	.06	1.97	44.80	36.23	2.10	1.30	97.42	.315
	10.04	.05	2.20	46.59	34.43	2.45	1.77	97.53	.282
	10.34	.05	2.08	46.50	36.00	2.04	1.35	98.37	.295
	10.44	.02	2.32	44.92	35.98	1.96	1.14	96.78	.308
	9.31	.04	1.97	48.16	35.56	1.76	1.11	97.91	.269
	9.33	.04	1.93	48.23	33.89	2.48	1.53	97.42	.259
*	10.19	.05	2.07	46.38	35.47	2.13	1.39	97.69	.291
	42.74	.02	.17	17.19	32.16	2.82	1.23	96.33	.82
	42.54	.04	.18	20.23	30.29	3.69	1.37	98.34	.78
	42.60	.02	.18	17.55	31.89	2.78	1.44	96.47	.81
	40.58	.03	.32	22.36	29.32	3.24	1.38	97.23	.76
*	42.12	.03	.21	19.33	30.92	3.13	1.36	97.10	.79
CP1-1G									
	10.47	.01	1.13	44.57	37.43	.39	1.54	95.54	.315
	10.77	0.00	1.11	44.36	37.82	.32	1.70	96.07	.322
	10.90	.01	1.10	44.12	37.95	.37	1.60	96.05	.326
	10.63	.01	1.11	44.52	37.42	.50	1.60	95.79	.317
	10.88	.03	1.30	43.31	37.58	.45	1.58	95.13	.331
	11.46	.02	1.08	42.54	38.20	.32	1.73	95.35	.346
	12.18	.01	1.21	41.70	39.10	.42	1.66	96.28	.365
	11.05	0.00	1.14	43.19	37.85	.42	1.49	95.14	.334
*	10.99	.01	1.13	43.74	37.89	.40	1.62	95.78	.330
	48.54	.01	.02	8.38	39.02	.88	3.02	99.87	.91
	49.56	0.00	.06	6.52	39.60	.93	3.27	99.93	.93
	48.75	0.00	.07	7.68	39.18	.86	3.09	99.63	.92
	49.31	0.00	.06	7.44	39.56	.88	3.17	100.43	.92
	48.38	.01	.07	9.47	38.19	1.28	3.00	100.40	.90
	48.03	.01	.09	8.63	38.43	.89	3.13	99.21	.91
	49.55	.01	.11	7.82	39.88	.90	3.03	101.30	.92
	48.02	.03	.11	8.43	38.51	.87	3.08	99.06	.91
-	48.86	.02	.10	7.55	39.32	.87	3.03	99.75	.92
*	48.81	.01	.07	8.00	39.12	.93	3.08	100.01	.92
CP1-2E									
	12.03	0.00	.92	42.40	38.84	.43	1.73	96.35	.355
	9.93	.01	.83	46.19	36.84	.33	1.78	95.91	.293
	11.24	0.00	1.01	43.45	38.00	.38	1.77	95.85	.335
	10.89	.02	.97	44.34	37.87	.38	1.66	96.13	.323
	11.59	0.00	1.01	44.17	36.75	1.67	1.68	96.87	.325
	10.14	.01	1.04	46.11	36.98	.60	1.65	96.53	.298
	10.54	0.00	.90	44.72	36.81	.41	2.14	95.52	.311
*	10.63	.01	.96	45.04	37.32	.55	1.74	96.25	.312
	47.51	.01	.05	9.66	37.95	.91	3.11	99.20	.90
	47.77	.01	.02	8.94	37.99	.93	3.27	98.93	.90
	47.89	.01	.04	7.80	38.38	.87	3.09	98.08	.92
	48.40	0.00	.31	8.73	37.99	1.25	3.26	99.94	.91
	47.51	.02	.02	9.21	37.67	1.01	3.21	98.65	.90
	47.60	.01	.18	8.41	37.04	.93	4.05	98.22	.91
	48.70	.02	.04	8.28	38.50	1.12	3.26	99.92	.91

	1.68	.02	.69	62.36	31.12	.08	.31	96.26	.051	
	1.71	.01	1.00	62.86	30.21	.63	.72	97.14	.050	
	3.46	.02	1.40	59.59	29.17	1.47	2.21	97.32	.094	
	2.84	.01	1.28	59.98	32.01	.06	.87	97.05	.087	
	2.85	.02	1.00	59.50	28.49	.87	2.54	95.27	.079	
	6.36	.02	1.60	54.95	32.40	1.68	1.88	98.89	.174	
	3.14	0.00	1.11	59.01	32.65	.10	.15	96.15	.098	
	1.96	0.00	1.37	61.60	29.90	.42	1.53	96.78	.058	
*	3.15	.01	1.21	59.78	30.91	.70	1.25	97.01	.091	
	42.82	.01	.14	17.80	32.49	1.53	3.25	98.03		.815
	38.59	.02	.25	29.84	22.43	4.25	4.64	100.02		.675
	38.53	.01	.15	26.38	27.19	2.18	3.53	97.96		.721
	33.51	.01	.70	33.93	23.44	1.42	4.11	97.12		.635
	37.77	0.00	.23	27.52	28.27	1.63	2.75	98.18		.714
	41.21	.01	.26	21.02	29.12	.99	6.10	98.71		.776
	40.88	.01	.22	20.93	29.80	2.15	3.09	97.08		.779
*	38.97	.01	.27	25.56	27.56	1.98	3.90	98.25		.730
BB8-200WR										
	10.20	.01	1.68	48.36	38.92	.26	1.88	101.32	.295	
	9.56	.03	1.40	49.80	38.36	.18	1.90	101.23	.275	
	8.89	.02	1.24	49.80	37.17	.01	2.06	99.19	.260	
	9.94	.02	1.51	48.50	38.09	.27	2.17	100.50	.287	
	9.93	.04	1.51	47.86	38.15	.03	2.24	99.76	.291	
	9.94	.04	1.45	48.67	38.58	.03	2.15	100.87	.288	
	9.39	.03	1.37	49.34	38.07	.03	1.92	100.14	.274	
	10.05	.03	1.68	48.44	38.78	.08	2.12	101.17	.292	
	7.98	.01	1.71	50.21	35.04	.10	2.89	97.94	.235	
*	9.69	.03	1.50	48.88	38.17	.12	2.08	100.47	.281	
	48.53	.02	.08	6.00	37.03	.11	6.33	98.10		.937
	47.76	.01	.08	8.07	34.49	.11	8.16	98.68		.914
	45.81	.01	.28	11.26	37.54	.19	3.27	98.37		.886
	47.97	.01	.07	7.38	38.41	.19	4.33	98.36		.925
	48.18	.01	.09	7.62	37.79	.13	5.24	99.05		.922
	48.30	.03	.09	7.05	36.96	.13	6.16	98.73		.927
	47.94	.03	.07	7.18	34.78	.13	8.00	98.13		.923
*	47.75	.02	.12	7.86	36.76	.14	5.85	98.51		.918
BB9-10C										
	6.81	.02	1.81	52.48	31.98	2.07	1.45	96.62	.191	
	9.26	.02	1.75	47.69	34.28	2.07	1.37	96.44	.263	
	9.53	.02	1.40	47.63	35.13	1.90	1.03	96.64	.271	
	8.56	.04	1.12	49.48	34.81	1.53	.92	96.46	.245	
*	8.48	.02	1.48	49.43	34.05	1.85	1.18	96.49	.241	
	40.33	.04	.30	20.87	31.42	1.72	1.76	96.44		.782
	41.39	.05	.28	20.39	31.73	1.89	2.09	97.82		.789
	47.18	.02	.28	9.19	36.67	2.41	1.44	97.19		.905
	36.49	.04	.45	29.38	26.32	2.67	1.71	97.06		.690
	43.46	.05	.30	13.77	34.46	1.77	1.45	95.26		.856
*	41.50	.04	.33	19.61	31.68	2.18	1.73	97.08		.796
GU3-23WR										
	11.04	.02	2.34	43.27	35.53	2.03	1.81	96.04	.324	
	9.66	.01	1.99	46.47	34.78	1.72	1.82	96.45	.280	
	12.53	.02	1.11	40.85	37.91	.63	2.64	95.68	.368	

	*	10.69	.01	1.96	44.26	35.63	1.63	1.96	96.14	.312	
		41.10	.01	.44	18.98	29.24	2.24	3.68	95.69		.794
		38.76	.01	.65	24.72	26.39	2.81	3.41	96.76		.732
		38.37	0.00	1.15	23.03	27.76	1.83	3.44	95.58		.749
	*	39.41	0.00	.75	22.27	27.78	2.30	3.51	96.02		.758
BB8-320WR		7.72	.01	1.64	52.42	36.48	.25	1.68	100.20	.226	
		5.98	0.00	1.31	55.77	33.85	.34	2.28	99.53	.170	
		7.94	.01	1.71	51.14	36.19	.24	1.86	99.08	.235	
	*	7.21	.01	1.55	53.10	35.51	.27	1.94	99.59	.210	
	*	48.11	0.00	.10	8.87	38.67	.78	3.16	99.69		.911
GU3-28WR		6.18	.03	3.54	52.75	33.44	.48	3.02	99.45	.188	
		8.12	.02	1.77	51.14	33.12	1.64	2.79	98.60	.222	
		6.49	.03	2.25	53.86	30.36	1.99	3.55	98.54	.172	
	*	6.91	.03	2.61	52.50	32.52	1.27	3.08	98.92	.196	
		35.55	.06	1.19	28.34	27.38	1.90	1.19	95.61		.699
		37.69	0.00	.35	26.10	25.73	2.30	4.01	96.19		.715
	*	36.97	.02	.63	26.86	26.27	2.17	3.07	95.99		.710
BB9-1C		7.42	.07	1.79	50.91	33.76	1.54	1.02	96.51	.217	
		10.36	.04	2.35	44.91	35.84	1.97	1.14	96.61	.306	
		8.36	.02	1.50	49.16	34.16	1.26	1.79	96.26	.242	
		8.56	0.00	2.00	48.13	34.43	1.72	.95	95.79	.253	
		9.43	.03	1.79	46.87	34.85	1.64	1.53	96.14	.274	
		9.46	.01	2.40	45.66	34.57	2.05	1.02	95.17	.283	
	*	8.79	.03	1.88	48.02	34.56	1.62	1.29	96.19	.257	
		41.33	.02	.28	19.72	30.96	2.38	1.94	96.63		.793
		34.20	.03	.61	32.20	25.49	1.38	2.77	96.68		.659
		41.98	.02	.34	18.98	31.46	2.41	1.97	97.16		.801
		37.84	.02	.41	26.70	27.29	2.56	2.15	96.97		.717
	*	39.47	.02	.39	23.32	29.33	2.23	2.16	96.92		.755
BB9-1WR		.87	0.00	.46	64.50	27.91	.11	2.76	96.61	.024	
		7.13	.02	1.15	51.53	33.56	.81	1.80	95.99	.207	
		9.53	.01	2.35	46.19	34.57	2.11	1.23	95.99	.280	
		8.43	0.00	2.63	47.98	33.56	2.19	1.12	95.92	.249	
	*	7.23	.01	1.94	50.91	32.85	1.60	1.56	96.09	.210	
		44.81	0.00	.56	13.26	34.53	2.14	1.93	97.23		.862
		41.17	0.00	.50	21.07	29.91	2.75	2.18	97.58		.778
		42.68	0.00	.53	15.04	33.87	1.01	2.68	95.81		.842
		37.50	0.00	.35	27.75	27.58	2.30	2.02	97.50		.709
	*	42.33	0.00	.50	17.91	32.11	2.13	2.13	97.11		.813
CP4-20BWR		5.61	.05	1.82	57.47	32.59	1.18	2.53	101.25	.152	
		6.12	.06	1.79	55.91	32.95	1.47	1.86	100.16	.168	
		5.87	.04	1.24	56.76	32.81	1.03	2.31	100.07	.159	
	*	5.87	.05	1.62	56.72	32.79	1.23	2.23	100.50	.160	
		40.53	.04	.15	24.88	28.30	2.61	3.45	99.96		.742
		40.18	.04	.15	24.06	28.50	2.55	3.05	98.53		.748
		44.67	.03	.09	15.06	33.08	1.50	4.36	98.79		.843
		42.04	.04	.13	20.93	30.49	2.15	3.44	99.22		.783

	40.89	.04	.18	24.08	29.15	2.74	2.70	99.78	.751
*	41.57	.04	.14	21.93	29.82	2.32	3.38	99.21	.772
GU3-17WR									
	10.39	.01	1.38	47.53	37.25	.11	3.55	100.22	.293
	10.07	.01	1.41	47.93	38.05	.20	2.24	99.90	.291
	9.67	0.00	1.88	47.60	36.19	.21	3.52	99.07	.280
*	10.04	.01	1.55	47.68	37.16	.17	3.10	99.72	.288
	49.81	0.00	.07	4.62	36.89	.09	7.64	99.12	.951
	49.60	0.00	.08	5.69	38.13	.13	6.16	99.79	.942
	49.09	0.00	.16	6.13	36.56	.21	7.12	99.26	.936
*	49.43	0.00	.11	5.57	37.01	.16	7.06	99.35	.942
GU3-20WR									
	10.39	0.00	1.22	47.50	38.48	.17	2.11	99.87	.300
	8.43	0.00	1.41	48.83	36.92	.08	1.05	96.72	.259
	10.04	0.00	1.92	48.43	39.12	.14	1.80	101.45	.295
	10.65	0.00	1.36	44.48	39.12	.24	.57	96.42	.328
*	9.92	0.00	1.39	47.20	38.33	.16	1.42	98.42	.296
	48.38	0.00	.05	7.18	37.98	.27	4.98	98.84	.926
	50.44	0.00	.08	4.10	38.14	.28	6.63	99.67	.958
	49.24	0.00	.04	7.14	37.48	.39	6.03	100.32	.927
	46.63	0.00	.13	10.25	36.91	.21	4.59	98.72	.895
*	49.28	0.00	.07	6.24	37.78	.30	5.92	99.60	.936
GU3-14WR									
	9.85	.04	1.25	45.64	37.42	.10	1.53	95.83	.301
	9.83	.06	1.31	46.94	37.60	.23	1.72	97.68	.293
	10.03	.02	1.62	45.79	36.85	.11	2.71	97.13	.300
*	9.87	.05	1.33	46.21	37.42	.16	1.78	96.82	.297
	47.72	.02	.06	6.46	39.14	.14	3.48	97.02	.934
	49.48	.02	.05	4.42	38.66	.29	5.25	98.17	.954
	49.05	0.00	.06	4.58	37.89	.13	5.91	97.62	.952
	47.74	.06	.08	7.39	39.44	.15	3.18	98.04	.925
*	48.44	.03	.06	5.76	38.82	.17	4.38	97.66	.941
BB8-85BWR									
	6.63	.02	1.04	54.05	33.93	.52	2.10	98.29	.188
	6.99	0.00	1.05	52.98	33.58	.68	2.33	97.61	.197
	6.85	.02	.98	54.27	33.83	.65	2.42	99.02	.190
	6.81	.01	.99	53.93	33.93	.57	2.24	98.48	.191
*	6.84	.01	1.01	53.78	33.81	.61	2.29	98.35	.192
	48.42	0.00	.19	8.14	37.59	1.04	4.05	99.43	.917
	46.54	0.00	.06	11.89	34.93	1.31	4.53	99.26	.877
	46.18	0.00	.03	12.66	34.40	1.33	4.70	99.30	.869
	47.97	0.00	.11	9.19	37.66	1.07	3.52	99.52	.907
*	47.33	0.00	.10	10.37	36.25	1.18	4.15	99.39	.894
GU3-11									
	8.42	.02	1.22	50.86	36.81	.25	1.62	99.20	.245
	10.02	.04	1.02	47.14	37.32	.23	2.21	97.97	.291
	8.58	.02	1.13	50.47	36.82	.27	1.62	98.92	.250
*	9.02	.02	1.11	49.45	36.98	.25	1.81	98.65	.262
	48.93	0.00	.11	7.61	39.03	.83	3.45	99.95	.924
	48.44	.02	.20	7.60	38.23	.80	3.85	99.14	.923
	48.42	.01	.25	7.54	38.51	.77	3.61	99.12	.923
	47.99	.01	.16	7.89	38.45	.85	3.15	98.50	.920

	*	48.52	.01	.17	7.64	38.63	.81	3.51	99.30		.923
GU3-31AWR		10.70	0.00	1.15	44.60	33.47	1.46	4.00	95.38		.294
		8.85	0.00	1.62	47.71	33.13	1.48	2.72	95.51		.251
		3.53	0.00	2.11	57.50	29.59	1.50	1.42	95.65		.102
	*	8.45	0.00	1.51	48.60	32.42	1.48	3.03	95.49		.237
	*	39.71	0.00	.64	22.08	28.32	2.98	2.05	95.78		.762
CP4-60WR		8.17	.08	1.37	50.35	36.35	.23	1.57	98.11		.243
		6.39	.06	1.14	54.07	34.56	.12	1.85	98.20		.187
		6.68	.08	.93	53.16	34.25	.11	2.15	97.36		.195
		7.80	.07	1.18	51.67	35.82	.19	1.96	98.69		.227
	*	7.26	.07	1.16	52.30	35.25	.16	1.88	98.08		.213
		43.74	.05	.03	17.02	36.02	.35	2.66	99.87		.831
		42.33	.02	.03	19.17	33.53	.73	3.19	99.00		.806
		45.79	0.00	.01	11.95	37.46	.40	2.97	98.58		.880
		44.96	.03	.02	13.59	36.54	.64	2.71	98.49		.863
	*	44.26	.02	.02	15.30	35.93	.54	2.87	98.94		.846
BB8-85B		6.39	.05	1.27	53.51	33.17	.50	2.39	97.28		.184
		6.66	.02	1.02	53.56	33.21	.57	2.55	97.59		.188
		6.84	.06	1.00	53.82	33.63	.64	2.45	98.44		.191
		6.71	.02	1.12	52.61	33.26	.52	2.32	96.56		.193
	*	6.64	.04	1.10	53.48	33.33	.56	2.44	97.59		.188
		49.02	0.00	.10	8.83	38.00	1.18	3.93	101.05		.912
		45.19	0.00	.13	14.72	33.90	1.37	4.24	99.56		.849
		49.54	.05	.11	6.15	39.15	.91	3.73	99.64		.938
		47.24	.02	.06	11.49	35.73	1.21	4.54	100.28		.883
		46.01	.01	.21	12.23	34.06	1.33	4.88	98.74		.872
	*	47.58	.02	.12	10.31	36.37	1.19	4.24	99.83		.895
BB8-100WR		3.82	.02	.65	59.07	32.22	.54	.72	97.04		.111
		5.56	0.00	.87	54.78	33.83	.01	1.39	96.44		.166
		2.13	0.00	.87	62.42	31.36	0.00	1.15	97.93		.063
		5.22	0.00	1.02	55.67	33.46	.17	1.37	96.92		.155
	*	4.79	0.00	.90	56.61	33.18	.14	1.27	96.89		.142
		46.83	0.00	.11	10.91	36.70	.42	4.60	99.57		.889
		48.44	0.00	.18	7.56	39.45	.50	3.18	99.31		.924
		48.25	0.00	.06	8.53	38.75	.42	3.84	99.86		.914
		46.97	0.00	.06	11.17	35.58	.66	5.41	99.85		.885
	*	47.57	0.00	.10	9.67	37.46	.51	4.35	99.66		.902
BB9-1A		1.19	.03	.51	63.11	27.98	.12	2.68	95.62		.033
		.11	.05	.24	65.37	25.57	.06	4.07	95.47		.003
		10.15	.04	1.46	44.83	37.27	.37	1.52	95.64		.310
	*	3.16	.04	.68	59.11	29.70	.17	2.74	95.59		.090
	*	35.53	.01	1.06	29.79	26.44	1.59	2.64	97.07		.684

	B09-1WR	B09-1A	B09-1B	B09-1C	B09-5C	B09-10A	B09-10C	B09-15WR	B09-25WR	B08-320WR	B08-200WR	B08-100WR
V	11	10	17	16	13	3	14	13	10	4	4	2
Cr	-	-	3	-	4	-	-	-	-	-	-	-
Co	.4	.1	.5	.6	.5	.2	.6	.6	.7	.2	.2	.2
Ni	<1	<1	<1	<1	2	<1	98	16	34	7	<1	33
Cu	5	10	3	4	4	4	7	4	5	7	3	4
Zn	78	19	121	124	82	31	116	63	58	47	43	47
Pb	30	25	40	40	15	5	10	20	25	45	40	25
Th	19.7	22.7	19.9	18.9	20.3	25.1	19.5	19.6	20.2	22.1	23.8	21.0
U	7.6	4.7	2.9	5.0	2.8	5.0	3.4	2.1	4.5	4.5	5.0	3.8

FROM SCHUARYTZ ET AL 1986
LLNL
N=72

	008-850wt	008-850	008-10	008-150	^{008-10E} 008-10	008-10WR	008-10	008-5	008-3A	008-30	008-2	008-1
V	3	-	2	2	2	2	2	1	1	2	1	1
Cr	-	-	6	5	1	3	2	2	1	2	1	1
Co	.2	.1	.2	.8	.3	.4	.9	.2	.3	.2	.2	.2
Ni	<1	-	6	8	6	6	6	6	6	6	6	6
Cu	3	20	5	13	10	20	19	6	15	22	40	36
Zn	45	50	46	59	49	46	49	40	51	61	47	61
Pb	20	20	25	45	25	25	30	25	30	15	30	20
Th	20.8	26.4	22.5	27.3	23.1	21.3	22.2	22.0	21.8	24.2	21.6	20.3
U	4.2	6.1	4.5	5.3	5.1	5.2	4.7	5.2	4.8	5.0	4.8	4.6

CP3-2a CP3-2b CP3-1WR CP3-1a CP3-1B CP3-1C CP3-1D CP4-20BWR CP4-60WR CP1-8WR CP1-9A CP1-2E CP1-16 CP1-AFB

V	12	12	8	2	1	3	7	8	5	2	1	2	1	2
Cr	6	5	4	4	4	5	10	-	-	2	4	3	1	2
Co	.7	.8	.5	.2	.6	.3	.6	.3	.2	.2	.2	.3	.2	.3
Ni	10	12	8	8	8	9	17	157	30	8	7	16	6	6
Cu	8	15	7	6	15	8	8	7	4	6	12	6	5	5
Zn	134	390	56	40	40	49	52	51	41	52	53	52	49	51
Pb	80	575	25	25	10	35	30	25	20	30	30	20	25	20
Th	19.0	20.8	21.1	22.2	20.0	23.5	21.6	23.0	20.2	24.5	22.7	22.7	23.4	24.3
U	2.3	2.2	3.6	6.1	4.6	4.5	2.6	4.8	1.2	4.9	4.9	4.3	4.7	5.7

CP1-AFWR	LW1-A	LW2-A	LW2-5	LW2-10	LW4-1A	LW4-1B	LW4-1C	LW4-5A	LW4-5B	LW4-10A	LW4-10B	LW4-15A
V	9	9	4	2	3	7	13	3	9	3	8	3
Cr	9	6	4	9	1	2	4	1	5	4	-	3
Co	.2	1.1	.5	.5	.3	.2	.6	1.1	.3	.7	.4	.5
Ni	6	17	12	10	13	8	9	10	8	8	8	24
Cu	6	12	8	19	8	12	22	12	8	30	20	23
Zn	52	65	63	53	39	45	57	66	37	60	46	40
Pb	2.5	20	15	15	35	25	20	25	30	25	25	20
Th	23.9	20.7	21.8	21.0	22.0	21.7	20.9	20.5	22.0	19.7	20.6	20.4
U	3.8	2.6	3.3	3.7	5.2	5.1	4.0	2.1	4.9	2.5	4.6	3.1

LW4-15B	LW4-5C	GU3-31BWR	GU3-31AWR	GU3-29WR	GU3-28WR	GU3-23WR	GU3-21WR	GU3-20WR	GU3-17WR	GU3-14WR	GU3-12	GU3-11	GU3-10	GU3-9
V	2	4	4	5	5	7	9	3	3	3	2	2	3	3
Cr	3	-	-	-	-	-	-	-	-	-	-	-	-	-
Co	.4	.7	.3	.4	.3	.3	.4	.1	.2	.2	.2	.2	.2	.2
Ni	8	8	<1	<1	2	<1	<1	<1	<1	5	<1	<1	16	<1
Cu	7	18	3	3	3	2	2	3	2	4	3	5	10	2
Zn	39	74	58	59	42	59	55	122	46	46	50	55	56	57
Pb	25	25	65	45	39	59	15	20	20	20	30	35	30	25
Th	22.0	18.4	25.8	28.0	21.8	20.8	21.6	22.3	22.7	23.1	23.3	21.7	22.3	21.5
U	5.2	2.8	2.4	3.3	3.1	3.6	4.3	3.3	3.7	4.4	4.4	4.5	4.4	3.5

	603-8	603-7	603-6	603-5	603-2	603-1
V	3	3	2	3	4.5	1
Cr	-	1	-	-	-	2
Co	.2	.2	.2	0	.1	.2
Ni	<1	<1	<1	<1	3	11
Cu	5	3	2	4	1	6
Zn	77	77	51	64	43	67
Pb	25	30	25	25	20	25
Mn	26.1	20.7	19.0	22.0	20.4	22.1
U	5.1	4.8	4.6	5.1	3.8	5.3

TOPOPAH SPRING MEMBERS

	<u>RANGE</u>	<u>AVERAGE</u>	<u>NUMBER OF SAMPLES</u>
V	0.5 - 17	5.0 5.0	70
Cr	1.0 - 41	4.4 4.4	40
Co	0.1 - 1.1	0.51 0.51	72
Ni	<1.0 - 157	10.7	71
Cu	10 - 40	9.4	72
Zn	19 - 390	61.5	72
Pb	5 - 575	34.1	72
Th	18.4 - 28.0	22.0	72
U	1.2 - 6.1	4.2	72

- DATA FROM SCHURAYTZ ET AL. (1986) INCLUDING BOTH WHOLE-ROCK AND INDIVIDUAL PUMICE ANALYSES
- ALL ANALYSES IN PPM